International Journal of Biological Macromolecules

Facile synthesis of starch and tellurium doped SrO nanocomposite for catalytic and antibacterial potential: in silico molecular docking studies

--Manuscript Draft--

Manuscript Number:	IJBIOMAC-D-22-05497R1
Article Type:	Research Paper
Section/Category:	Carbohydrates, Natural Polyacids and Lignins
Keywords:	Strontium oxide; Starch; Composite
Corresponding Author:	Muhammad Ikram Government College University Lahore Department of Physics Lahore, Pakistan PAKISTAN
First Author:	Muhammad Ikram
Order of Authors:	Muhammad Ikram
	Ali Haider
	Muhammad Imran
	Junaid Haider
	Sadia Naz
	Anwar Ul-Hamid
	Walid Nabgan
	Muhammad Mustajab
	Anum Shahzadi
	Iram Shahzadi
	Muhammad Asif Raza
	Ghazanfar Nazir
Abstract:	A chemical co-precipitation route was used to synthesize novel strontium oxide (SrO), SrO-starch composite and various tellurium (Te) concentrations were incorporated in SrO-starch composite. This study aims to enhance the catalytic activities and bactericidal behavior of SrO, SrO-starch composite with different percentage concentrations of Te doping and a fixed amount of starch nanoparticles. XRD affirmed that the dopant contribution was investigated to improve crystallinity. Surface morphological characteristics and elemental composition evaluation were determined using an FE-SEM and EDS exhibit a doping concentration of an element in the synthesized products. The configuration of Sr–O–Sr bonds and molecular vibrations has been indicated by FTIR spectra. In addition, dye degradation of prepared samples was investigated through catalytic activity (CA) in the existence of NaBH4 act as a reduction representative. The Te-doped SrO-starch composite indicates superior catalytic activity and shows a degradation of Methylene blue dye (91.4%) in an acidic medium. The synthesis nanocatalyst demonstrated impressive antibacterial activity against Staphylococcus aureus (S. aureus) at high and low concentrations exhibiting zones of inhibition 9.30 mm as compared to ciprofloxacin. Furthermore, molecular docking studies of synthesized nanocomposites were performed against selected enzyme targets, i.e., β-lactamaseE.coli and DNA GyraseE.coli.
Suggested Reviewers:	Dayong Wu dayongwu@mail.ipc.ac.cn
	Muhammad Maqbool mmaqbool@uab.edu
	Alberto Naldoni alberto.naldoni@upol.cz

Opposed Reviewers:	
Response to Reviewers:	Reviewer's Responses to Questions Reviewer #1: This study aims to enhance the catalytic activities and bactericidal behavior of SrO, SrO-starch composite with different percentage concentrations of Te doping and a fixed amount of starch nanoparticles. The suggestions: 1. SrO and starch were introduced in the "Introduction" section of the article, but Te is not referred. And the authors can add an introduction to Te in this section to help readers better understand the article. Ans: The introduction regarding Te has been added on pages 4 and 5, lines 85-96. ---------- 2. If applicable, is the method/study reported in sufficient detail to allow for its replicability and/or reproducibility? Please provide suggestions to the author(s) on how to improve the replicability/reproducibility of their study. Please number each suggestion so that the author(s) can more easily respond. Reviewer #1: Mark as appropriate with an X: Yes [X] No [] N/A [] Provide further comments here: These methods are well described and enough for the determination of the catalytic and bactericidal activities, but lacking of depth and innovation. The suggestions: 1. Studies have demonstrated that nano-Te has excellent antibacterial activity and catalytic performance. In the study of antibacterial activity and catalytic activity in this article, the grouping does not comprise the individual research of nano-Te. How to determine whether the enhancement of catalytic activities and bactericidal behavior is due to the combined effect of Te/SrO-starch composite NPs or the effect of nano-Te? Ans.: We have performed catalytic and antimicrobial activity with combine effect of Te/SrO-starch composite with variation in concentration of Te that shows the effect of nano-Te in both catalytic and antimicrobial activity. The Te-doped nanocomposites have excellent catalytic and antimicrobial at an optimum concentration of Te (2 and 4%). ---------- 3. If applicable, are statistical analyses, controls, sampling mechanism, and statistical reporting (e.g., P-values, CIs, effect sizes) appropriate and well described? Please clearly indicate if the manuscript requires additional peer review by a statistician. Kindly provide suggestions to the author(s) on how to improve the statistical analyses, controls, sampling mechanism, or statistical reporting. Please number each suggestion so that the author(s) can more easily respond. Reviewer #1: Mark as appropriate with an X: Yes [X] No [] N/A [] Provide further comments here: The suggestions: 1. The significance of difference is not mentioned in this paper, and the authors should be modified. Ans.: The significance of difference is modified in abstract and conclusion. ---------- 4. Could the manuscript benefit from additional tables or figures, or from improving or removing (some of the) existing ones? Please provide specific suggestions for improvements, removals, or additions of figures or tables. Please number each suggestion so that author(s) can more easily respond. Reviewer #1: The suggestions: 1. Fig. 2. Schematic description of catalytic performance. In this figure, “H20” should be corrected to “H2O”. Ans.: Corrected; see Fig. 2 on page 9.

2. Fig. 5. calculated interlayer d-spacing using the HR-TEM micrograph of a) SrO, b) SrO-starch, c) Te (2 %), and d) Te (4 %) samples. The first letter of the captions should be capitalized.
Ans.: Revised as per suggestion on page 18, lines 284 and 285.

---

5. If applicable, are the interpretation of results and study conclusions supported by the data?

Please provide suggestions (if needed) to the author(s) on how to improve, tone down, or expand the study interpretations/conclusions. Please number each suggestion so that the author(s) can more easily respond.

Reviewer #1: Mark as appropriate with an X:
Yes [X] No [] N/A []
Provide further comments here: The paper made a systemic study and the results is believable.
The suggestions:
1. The interpretation of the results and discussion are considered to be oversimplified. In-depth data mining to the result is recommended.

Ans.: We have modified the results and discussion.
2. The catalytic activity and bactericidal activity of Te/SrO-starch composite NPs should be more combined with their nanostructures.
Ans.: Modified catalytic and antimicrobial activity of NPs with nanostructures.

---

6. Have the authors clearly emphasized the strengths of their study/methods?

Please provide suggestions to the author(s) on how to better emphasize the strengths of their study. Please number each suggestion so that the author(s) can more easily respond.

Reviewer #1: To study the catalytic activities and bactericidal behavior of Te/SrO-starch composite NPs, the characterization of Te/SrO-starch composite NPs were firstly studied by XRD, FE-SEM, FTIR, and PL spectroscopy. Secondly, the authors chose Escherichia coli (E. coli) and Staphylococcus aureus (S. aureus) as the object to study the bactericidal activities. Finally, two enzyme targets (β-lactamaseE.coli and DNA GyraseE.coli) were selected to explore the molecular docking studies.

---

7. Have the authors clearly stated the limitations of their study/methods?

Please list the limitations that the author(s) need to add or emphasize. Please number each limitation so that author(s) can more easily respond.

Reviewer #1: Molecular docking studies suggested these nanocomposites as potential inhibitors of β-lactamaseE.coli and DNA GyraseE.coli, further study work is needed to be done in case applicable.
Ans: We selected β-lactamaseE.coli and DNA GyraseE.coli as possible targets for exploring the inhibitory potential of these nanocomposites. These findings are in silico predictions and studies like Enzyme inhibition analysis are beyond the scope of current study and suggested to be explored in future.

---

8. Does the manuscript structure, flow or writing need improving (e.g., the addition of subheadings, shortening of text, reorganization of sections, or moving details from one section to another)?

Please provide suggestions to the author(s) on how to improve the manuscript structure and flow. Please number each suggestion so that author(s) can more easily respond.

Reviewer #1: The suggestions:
1. The methods of "2.2 Synthesis of Strontium oxide" and "2.2.1 Synthesis of Starch and Te/ SRO-starch composite" should be combined. And the focus of the subheading

	should be synthesis of starch and Te/ Sro-starch composite rather than synthesis of strontium oxide. Ans: We have combined the synthesis portion as the reviewer's suggestion with the heading of “Synthesis of starch and Te/SrO-starch composite” on pages 6 and 7. 2. The conclusion needs to be more concise. Ans: we have modified the conclusion. --- 9. Could the manuscript benefit from language editing? Reviewer #1: Yes Reviewer #1: The manuscript is well written and well organized. However, there are still some areas of the article that need to be revised： 1. Line 21 and 23 on the page 7, "ul" and "ml" should be changed to "uL" and "mL". Similar errors should be carefully checked and corrected. Ans: The change regarding uL and mL was done as the reviewer's suggestions throughout the article. 2. Line 27 on page 2, "Molecular vibrations" should be modified to "molecular vibrations". Ans: "Molecular vibrations" modified to "molecular vibrations" on page 2, line 30 3. Line 46 on page 4, line 37 on page 12 and line 7 on page 15, "structures[17]", "(c)SAED pattern" and "SrO-starch composited) 2% Te" should add a blank space. Ans: Suggested modification for blank space at Line 84 on page 4, line 228 on page 13 and lines 265 and 266 on page 17. 4. Line 48 on page 7, "the equation % Degradation = C0−Ct /C0 × 100" should be annotated. Ans: % Degradation = C0−Ct /C0 × 100" was annotated at page 8 and line 148-150. 5. Line 58 on page 8 and line 4 on page 9, "E. coli" and "S. aureus" should be italicized. Similar errors should be carefully checked and corrected. Ans: "E. coli" and "S. aureus" has been modified to italic throughout the manuscript. 6. Line 36 on page 8 and line 16 on page 9, "24 h" and "24 hours", you should be uniform. Ans: “24 h” changed to “24 hours” uniformly on page 9, line 156. 7. Line 27 and line 33 on page 9, "2.6. Molecular Docking Studies:" and "antibacterial agents. ," should be corrected. Ans: Suggested modification was corrected on page 10, lines 174 and 176. 8. Line 34 and line 36 on page 10, "SrO-starch" and "SrO-Starch", you should be uniform. Ans: Uniformly changed to “SrO-starch” on page 11, line 199 and throughout the manuscript. 9. Line 36 on page 13, whether "SRO-starch NSs composite material" is wrong? "SRO-starch NSs composite material" is not involved in this paper. Ans: Thanks for the suggestion; we have revised the manuscript and changed to “SrO-starch composite” 10. Some journal names in "References" are abbreviated and some are not, you should be uniform. Also the page numbers of the journals are not displayed. Ans: Uniformly changed and also displayed the page number of the journals.

Editor-in-Chief
International Journal of Biological Macromolecules
Dear Editor,
We are submitting our manuscript entitled “Facile synthesis of starch and tellurium doped SrO nanocomposite for catalytic and antibacterial potential: in silico molecular docking studies” by authors for review and, if acceptable, for publication in International Journal of Biological Macromolecules.

This paper contains evidence and discussion of Strontium oxide (SrO), SrO-starch composite, and varied tellurium (Te) concentrations were synthesised through chemical co-precipitation. Surface morphology and elemental composition examination using FE-SEM and EDS show doping in manufactured goods. Doping elements, phase composition, and crystallinity were confirmed by XRD. Dopant addition improves particle crystallinity and crystallite size. SAED profiles showed significant crystallinity and sharp peaks, matching XRD data. FTIR spectra show Sr–O–Sr bonds and molecular vibrations. UV-vis spectroscopy of SrO and Te/SrO-starch samples showed a transfer in absorbance to the infrared (blue shift), owing to an increase in energy bandgap. Photoluminescence (PL) spectroscopy examines charge carrier movement, trapping efficiency, and electron-hole recombination behaviour. This paper attempts to improve the catalytic activities of SrO, SrO-starch composite with varying Te doping percentages and a set number of starch nanoparticles (NPs). Dye degradation of prepared samples was also evaluated using catalytic activity (CA) using $NaBH_4$ as a reduction representative. Te-doped SrO-starch composite shows better catalytic activity than virgin SrO and SrO-starch composite. At high and low concentrations, the synthesised nanocatalyst showed antibacterial efficacy against S. aureus. Synthesized nanocomposites were docked against -lactamaseE.coli and DNA GyraseE.coli. As such, we believe this manuscript would be of interest to those working in the field and is suitable for International Journal of Biological Macromolecules.
The manuscript, or its contents in some other form, has not been published previously by any of the authors and/or is not under consideration for publication in another journal at the time of submission. In the hope you will find this article worthy of publication in your prestigious journal and thanking you in anticipation. Thank you.
Two day ago, I submitted this manuscript in Applied Surface Sciences and Editor recommended your prestigious Journal.

Sincerely,

Dr. M. Ikram

Reviewer's Responses to Questions

Reviewer #1: This study aims to enhance the catalytic activities and bactericidal behavior of SrO, SrO-starch composite with different percentage concentrations of Te doping and a fixed amount of starch nanoparticles.
The suggestions:
1. SrO and starch were introduced in the "Introduction" section of the article, but Te is not referred. And the authors can add an introduction to Te in this section to help readers better understand the article.

Ans: The introduction regarding Te has been added on pages 4 and 5, lines 85-96.

---

2. If applicable, is the method/study reported in sufficient detail to allow for its replicability and/or reproducibility?

Please provide suggestions to the author(s) on how to improve the replicability/reproducibility of their study. Please number each suggestion so that the author(s) can more easily respond.

Reviewer #1: Mark as appropriate with an X:
Yes [X] No [] N/A []
Provide further comments here: These methods are well described and enough for the determination of the catalytic and bactericidal activities, but lacking of depth and innovation.
The suggestions:
1. Studies have demonstrated that nano-Te has excellent antibacterial activity and catalytic performance. In the study of antibacterial activity and catalytic activity in this article, the grouping does not comprise the individual research of nano-Te. How to determine whether the enhancement of catalytic activities and bactericidal behavior is due to the combined effect of Te/SrO-starch composite NPs or the effect of nano-Te?

Ans.: We have performed catalytic and antimicrobial activity with combine effect of Te/SrO-starch composite with variation in concentration of Te that shows the effect of nano-Te in both catalytic and antimicrobial activity. The Te-doped nanocomposites have excellent catalytic and antimicrobial at an optimum concentration of Te (2 and 4%).

---

3. If applicable, are statistical analyses, controls, sampling mechanism, and statistical reporting (e.g., P-values, CIs, effect sizes) appropriate and well described?

Please clearly indicate if the manuscript requires additional peer review by a statistician. Kindly provide suggestions to the author(s) on how to improve the statistical analyses, controls, sampling mechanism, or

statistical reporting. Please number each suggestion so that the author(s) can more easily respond.

Reviewer #1: Mark as appropriate with an X:
Yes [X] No [] N/A []
Provide further comments here:
The suggestions:
1. The significance of difference is not mentioned in this paper, and the authors should be modified.

Ans.: The significance of difference is modified in abstract and conclusion.

---

4. Could the manuscript benefit from additional tables or figures, or from improving or removing (some of the) existing ones?

Please provide specific suggestions for improvements, removals, or additions of figures or tables. Please number each suggestion so that author(s) can more easily respond.

Reviewer #1: The suggestions:
1. Fig. 2. Schematic description of catalytic performance. In this figure, “H20” should be corrected to “H2O”.

Ans.: Corrected; see Fig. 2 on page 9.
2. Fig. 5. calculated interlayer d-spacing using the HR-TEM micrograph of a) SrO, b) SrO-starch, c) Te (2 %), and d) Te (4 %) samples. The first letter of the captions should be capitalized.

Ans.: Revised as per suggestion on page 18, lines 284 and 285.

---

5. If applicable, are the interpretation of results and study conclusions supported by the data?

Please provide suggestions (if needed) to the author(s) on how to improve, tone down, or expand the study interpretations/conclusions. Please number each suggestion so that the author(s) can more easily respond.

Reviewer #1: Mark as appropriate with an X:
Yes [X] No [] N/A []
Provide further comments here: The paper made a systemic study and the results is believable.
The suggestions:

1. The interpretation of the results and discussion are considered to be oversimplified. In-depth data mining to the result is recommended.

Ans.: We have modified the results and discussion.

2. The catalytic activity and bactericidal activity of Te/SrO-starch composite NPs should be more combined with their nanostructures.

Ans.: Modified catalytic and antimicrobial activity of NPs with nanostructures.

---

6. Have the authors clearly emphasized the strengths of their study/methods?

Please provide suggestions to the author(s) on how to better emphasize the strengths of their study. Please number each suggestion so that the author(s) can more easily respond.

Reviewer #1: To study the catalytic activities and bactericidal behavior of Te/SrO-starch composite NPs, the characterization of Te/SrO-starch composite NPs were firstly studied by XRD, FE-SEM, FTIR, and PL spectroscopy. Secondly, the authors chose Escherichia coli (E. coli) and Staphylococcus aureus (S. aureus) as the object to study the bactericidal activities. Finally, two enzyme targets (β-lactamaseE.coli and DNA GyraseE.coli) were selected to explore the molecular docking studies.

---

7. Have the authors clearly stated the limitations of their study/methods?

Please list the limitations that the author(s) need to add or emphasize. Please number each limitation so that author(s) can more easily respond.

Reviewer #1: Molecular docking studies suggested these nanocomposites as potential inhibitors of β-lactamaseE.coli and DNA GyraseE.coli, further study work is needed to be done in case applicable.

Ans: We selected β-lactamase$_{E.coli}$ and DNA Gyrase$_{E.coli}$ as possible targets for exploring the inhibitory potential of these nanocomposites. These findings are in silico predictions and studies like Enzyme inhibition analysis are beyond the scope of current study and suggested to be explored in future.

---

8. Does the manuscript structure, flow or writing need improving (e.g., the addition of subheadings, shortening of text, reorganization of sections, or moving details from one section to another)?

Please provide suggestions to the author(s) on how to improve the manuscript structure and flow. Please number each suggestion so that author(s) can more easily respond.

Reviewer #1: The suggestions:
1. The methods of "2.2 Synthesis of Strontium oxide" and "2.2.1 Synthesis of Starch and Te/ SRO-starch composite" should be combined. And the focus of the subheading should be synthesis of starch and Te/ Sro-starch composite rather than synthesis of strontium oxide.

Ans: We have combined the synthesis portion as the reviewer's suggestion with the heading of "Synthesis of starch and Te/SrO-starch composite" on pages 6 and 7.
2. The conclusion needs to be more concise.

Ans: we have modified the conclusion.

---

9. Could the manuscript benefit from language editing?

Reviewer #1: Yes

Reviewer #1: The manuscript is well written and well organized. However, there are still some areas of the article that need to be revised：
1. Line 21 and 23 on the page 7, "ul" and "ml" should be changed to "uL" and "mL". Similar errors should be carefully checked and corrected.

Ans: The change regarding uL and mL was done as the reviewer's suggestions throughout the article.
2. Line 27 on page 2, "Molecular vibrations" should be modified to "molecular vibrations".

Ans: "Molecular vibrations" modified to "molecular vibrations" on page 2, line 30
3. Line 46 on page 4, line 37 on page 12 and line 7 on page 15, "structures[17]", "(c)SAED pattern" and "SrO-starch composited) 2% Te" should add a blank space.

Ans: Suggested modification for blank space at Line 84 on page 4, line 228 on page 13 and lines 265 and 266 on page 17.
4. Line 48 on page 7, "the equation % Degradation = C0−Ct /C0 × 100" should be annotated.

Ans: % Degradation = C0−Ct /C0 × 100" was annotated at page 8 and line 148-150.
5. Line 58 on page 8 and line 4 on page 9, "E. coli" and "S. aureus" should be italicized. Similar errors should be carefully checked and corrected.

Ans: "*E. coli*" and "*S. aureus*" has been modified to italic throughout the manuscript.

6. Line 36 on page 8 and line 16 on page 9, "24 h" and "24 hours", you should be uniform.

Ans: “24 h” changed to “24 hours” uniformly on page 9, line 156.

7. Line 27 and line 33 on page 9, "2.6. Molecular Docking Studies:" and "antibacterial agents. ," should be corrected.

Ans: Suggested modification was corrected on page 10, lines 174 and 176.

8. Line 34 and line 36 on page 10, "SrO-starch" and "SrO-Starch", you should be uniform.

Ans: Uniformly changed to “SrO-starch” on page 11, line 199 and throughout the manuscript.

9. Line 36 on page 13, whether "SRO-starch NSs composite material" is wrong? "SRO-starch NSs composite material" is not involved in this paper.

Ans: Thanks for the suggestion; we have revised the manuscript and changed to “SrO-starch composite”

10. Some journal names in "References" are abbreviated and some are not, you should be uniform. Also the page numbers of the journals are not displayed.

Ans: Uniformly changed and also displayed the page number of the journals.

Declaration of interests/Conflict of Interest

☒ The authors declare that they have no known competing financial interests or personal relationships that could have appeared to influence the work reported in this paper.
This manuscript has no conflict of interest

Dr. Muhammad Ikram
Assistant Professor Physics
GC University Lahore

Author Statement

Muhammad Ikram, Conceptualization, Supervision

Ali Haider, Methodology and Writing

Muhammad Imran, Review and Editing

Junaid Haider, Software and Formal Analysis

Sadia Naz, Data Curation and writing

Anwar Ul-Hamid, Resources and Review and Editing

Walid Nabgan, Review and Editing

Muhammad Mustajab, Writing

Anum Shahzadi, Software and Formal Analysis

Iram Shahzadi, Validation and Investigation

Muhammad Asif Raza, Methodology

Ghazanfar Nazir, Review and Editing

Facile synthesis of starch and tellurium doped SrO nanocomposite for catalytic and antibacterial potential: in silico molecular docking studies

Muhammad Ikram[a], Ali Haider[b], Muhammad Imran[c], Junaid Haider[d], Sadia Naz[d], Anwar Ul-Hamid[e], Walid Nabgan[f*], Muhammad Mustajab[a], Anum Shahzadi[g], Iram Shahzadi[h], Muhammad Asif Raza[i], Ghazanfar Nazir[j]

[a]Solar Cell Applications Research Lab, Department of Physics, Government College University Lahore, 54000, Pakistan

[b]Department of Clinical Sciences, Faculty of Veterinary and Animal Sciences, Muhammad Nawaz Shareef University of Agriculture, Multan, 66000, Pakistan

[c]Department of Chemistry, Government College University Faisalabad, Pakpattan Road, Sahiwal, Punjab, 57000, Pakistan

[d]Tianjin Institute of Industrial Biotechnology, Chinese Academy of Sciences, Tianjin 300308, China.

[e]Core Research Facilities, King Fahd University of Petroleum & Minerals, Dhahran, 31261, Saudi Arabia

[f]Departament d'Enginyeria Química, Universitat Rovira i Virgili, Av Països Catalans 26, 43007 Tarragona, Spain

[g]Faculty of Pharmacy, The University of Lahore, Lahore, Pakistan

[h]Punjab University College of Pharmacy, University of the Punjab, 54000, Pakistan

[i]Department of Pathobiology, Faculty of Veterinary and Animal Sciences, Muhammad Nawaz Shareef University of Agriculture, Multan, 66000, Pakistan

[j]Department of Nanotechnology and Advanced Materials Engineering, Sejong University, Seoul, Republic of Korea

*Corresponding author email: [a]dr.muhammadikram@gcu.edu.pk, [f]wnabgan@gmail.com

ABSTRACT

A chemical co-precipitation route was used to synthesize novel strontium oxide (SrO), SrO-starch composite and various tellurium (Te) concentrations were incorporated in SrO-starch composite. This study aims to enhance the catalytic activities and bactericidal behavior of SrO, SrO-starch composite with different percentage concentrations of Te doping and a fixed amount of starch nanoparticles. XRD affirmed that the dopant contribution was investigated to improve crystallinity. Surface morphological characteristics and elemental composition evaluation were determined using an FE-SEM and EDS exhibit a doping concentration of an element in the synthesized products. The configuration of Sr–O–Sr bonds and molecular vibrations has been indicated by FTIR spectra. In addition, dye degradation of prepared samples was investigated through catalytic activity (CA) in the existence of $NaBH_4$ act as a reduction representative. The Te-doped SrO-starch composite indicates superior catalytic activity and shows a degradation of Methylene blue dye (91.4%) in an acidic medium. The synthesis nanocatalyst demonstrated impressive antibacterial activity against *Staphylococcus aureus* (*S. aureus*) at high and low concentrations exhibiting zones of inhibition 9.30 mm as compared to ciprofloxacin. Furthermore, molecular docking studies of synthesized nanocomposites were performed against selected enzyme targets, i.e., β-lactamase$_{E.coli}$ and DNA Gyrase$_{E.coli}$.

Keywords: Strontium oxide; starch; composite

1. INTRODUCTION

Freshwater resources all around the globe are becoming susceptible to pollution and depleting as a consequence of anthropogenic activities in various industrial sectors, particularly in textile mills. Pesticides and industrial chemical waste have been dumped into rivers, lakes, and coastlines regularly, owing to contamination of water supplies worldwide [1]. The world is facing massive challenges in achieving the increasing demands for used water as freshwater sources are constantly depleting due to an increase in population growth, prolonged water shortages, public health initiatives, and competing requirements from a diverse range of consumers [2–4]. Bacterial contamination in drinkable water is suspected of promoting a significant portion of general health conditions in developing countries such as Pakistan. Some of the most common methods for purifying contaminated water include the use of physical and chemical intermediaries containing chlorine and its derivatives, low-frequency ultrasound, activated carbon, reverse osmosis, heating, ultra-violet radiation, solid stone, water sediment filters including ceramics and fibers, distillation, catalysis and photocatalysis activity, filtered water, pitcher and roller filter, ozone exchange softener and water ion exchange [5,6]. Human diseases, such as hepatitis, diarrhea, cryptosporidiosis, encephalitis, leptospirosis, and typhoid fever, are spreading because of contaminated water. Globally, 1.4 million cases of hepatitis A are diagnosed yearly, with a mortality rate of 12 800 to 16 100 [7]. Hazardous contaminants in effluent contain both inorganic and organic toxic metals and dangerous solvents and compounds, all of which must be primarily decayed to attain a sustainable green environment [8].

Metal oxide nanomaterials have been used in various applications for water and wastewater treatment. The non-magnetic behavior of strontium oxide (SrO) with a large energy band gap of alkali earth metal-based oxide with a cubic structure similar to sodium chloride (NaCl) structure.

SrO has been used as a catalyst in the field of microelectronics. Several polymer-based metal oxide composites, including SrO, have recently been modified to improve the catalytic properties of metal oxide nanomaterials [9]. Strontium oxides have been used in various biomedical processes, including therapeutic implant cement, tissue or body elements replacement, and compound filling. Because of their biodegradability, predictability, abundant supply, relatively inexpensive, and recycled content within and between polymers such as cellulose and starch polymers are relatively competitive applicants for synthesizing polymeric composites [10,11]. Moreover, the negligible antimicrobial activity of polymers restricts their use in recycling food, water, and wastewater treatment. Polymeric composite materials with appropriate doping can substantially enhance their catalytic potential and antimicrobial properties [12]. Starch is a carbohydrate polymeric abundant in our diet [13]. Starch is a polysaccharide polymer with a high molecular weight that can be extracted from plants composed of amylose and amylopectin and has been found in a wide variety of crop production potato tubers, cassava roots, and corn kernels. Starch is a low-cost, biologically sustainable energy raw material source for the nutrition, paper, chemical, and pharmaceutical industries [14–16]. Starch nanoparticles (NPs) with the size of particle in 20-50 nm range has been generated by the formation of complexes of starch–butanol constructions accompanied by hydrolysis process of enzymes for starch–butanol structures [17]. Starch-based nanocomposite materials have been used in the food service sector to grow alternate methodologies to preserve and help perpetuate smell and taste [18]. Semimetal oxide nanoparticles belong to a class of nanostructured materials with unique features that enable their usage in various processes, such as catalysis. Tellurium (Te)-doped compounds and alloys are of particular interest to researchers among the various types of chalcogenide materials due to the possible technological applications to be developed with these materials [19]. Tellurium

oxide (TeO_2) is a p-type chalcogenide material that can exist in both crystalline and amorphous phases. It has a broadband gap. TeO_2 can be found in both the paratellurite (tetragonal) and tellurite (orthorhombic) phases when it is in crystalline form [20]. TeO_2 is versatile due to its amazing qualities, which include its great chemical stability, mechanical durability, high refractive index, good optical non-linearity, and high electrical conductivity. These properties make TeO_2 appropriate for a wide range of applications [21] catalytic and antimicrobial activity. The fabrication of Te/starch-doped SrO NPs and their implementations in organic and inorganic pollutant degradation and antibacterial activity have yet to be reported. A chemical co-precipitation route has been adopted to doping Te and starch into SrO to form Te/SrO-starch composite NPs and illustrate that Te/SrO-starch composite NPs improved the catalytic activity for degradation of dye and antimicrobial activity. Furthermore, Te and starch-doped consequences on SrO characteristics such as optical, surface, structural morphology, crystallinity, and chemical composition have been discussed and investigated. Computational techniques facilitate researchers to explore in-depth mysteries behind various biological activities. Here, we selected two enzymes from cell wall synthesis and nucleic acid synthesis pathways, i.e., β-lactamase$_{E.coli}$ and DNA Gyrase$_{E.coli}$, respectively and performed molecular docking predictions for the understanding binding tendency of synthesized nanocomposites against them.

2. Experimental sections

2.1 Materials

Strontium chloride hexahydrate ($SrCl_2.6H_2O$, 99%), tellurium dioxide (TeO_2, 99%), and sodium hydroxide (NaOH, 98%) has been purchased from sigma Aldrich Germany. Starch (99.6%) was procured from Sigma Aldrich Japan. All materials were used without further purification.

2.2 Synthesis of starch and Te/SrO-starch composite

The chemical co-precipitation method was used to prepare the control sample of 0.5 M solution of SrO by using $SrCl_2.6H_2O$ under constant heating and stirring at 90 °C for one hour to get a homogeneous mixture. 0.5 M solution of NaOH has been utilized to maintain pH~ 12 of the synthesized solution. The prepared precipitates were filtered and washed with de-ionized water (DI water) to remove the residual reaction mixture. After centrifugation at 7500 rpm, the prepared specimens were heated for 24 hours at 120 °C and grinded to get fine powder, as revealed in Fig. 1.

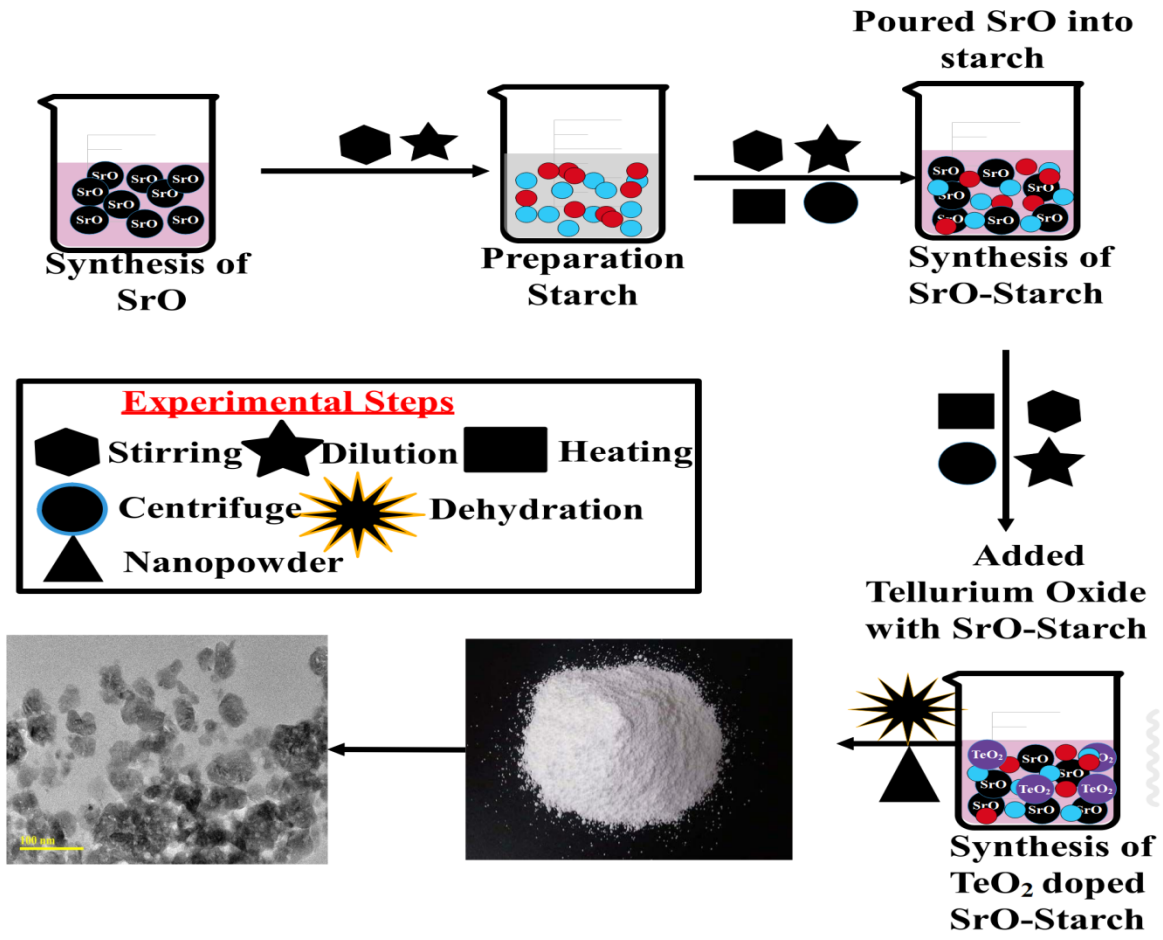

120

121 **Fig.1** Schematic synthesis illustration to fabricate Te/SrO-starch nanoparticles.

122 3g of starch and a fixed amount of distilled water (85 mL) were poured into a beaker, stirred and
123 heated for 1 hour at 70 °C, and grind the material. To avoid infestation, the powdered product
124 was stored in an airtight desiccator. To synthesize the required composite nanomaterials, an
125 appropriate starch concentration was solubilized into a $SrCl_2.6H_2O$ solution at pH~12.
126 The various concentration of TeO_2 (2 and 4 %) under constant heating and stirring has been
127 incorporated. The prepared specimens have been heated and stirred at 90 °C for 30 minutes. The
128 precipitates accumulated by centrifugation at 7500 rpm and repetitively cleaned with DI water.

The precipitates have been heated overnight at 120 °C to yield fine dust of Te/SrO-starch composite nanomaterials indicated in Fig. 1.

2.3 Catalytic activity

To test the catalytic properties of the synthesized catalysts, methylene blue (MB) dye solution has been prepared in 1000 mL of DI water by dissolving 0.005 g of MB. To acquire a homogeneous mixture, the solution was placed in the dark, continuous stirring for 20 min. In the dark, a 0.1 M $NaBH_4$ solution act as a reducing agent was prepared in DI water. A 200 µL $NaBH_4$ solution has been transferred into a dye (3 mL) concentration. Then the solution was dubbed the "blank sample (without nanocatalyst)," dye degradation assessed. The mechanism of dye degradation is represented in Fig.2. The catalytic activity (CA) has been measured by incorporating 400 µL of prepared catalyst into the same mixture (dye and $NaBH_4$ solution). The transformation of color of dye from blue to colorless dye solution demonstrated that the degradation of dye had been successfully adopted. The prepared samples have been examined using UV–Vis spectrophotometry to measure the degree of dye degradation in a specific time interval. Furthermore, the CA has been calculated in three different media, namely acidic by using H_2SO_4 with pH ~3, neutral with pH ~7, and basic solution has been made with the help of NaOH to adjust the pH~12, respectively. The percentage of dye degradation for each sample has been computed from the equation % Degradation = $C_0 - C_t / C_0 \times 100$, where C_0 is the initial concentration of dye at t0 and C_t is the final concentration of dye at t after incorporation of composite materials.

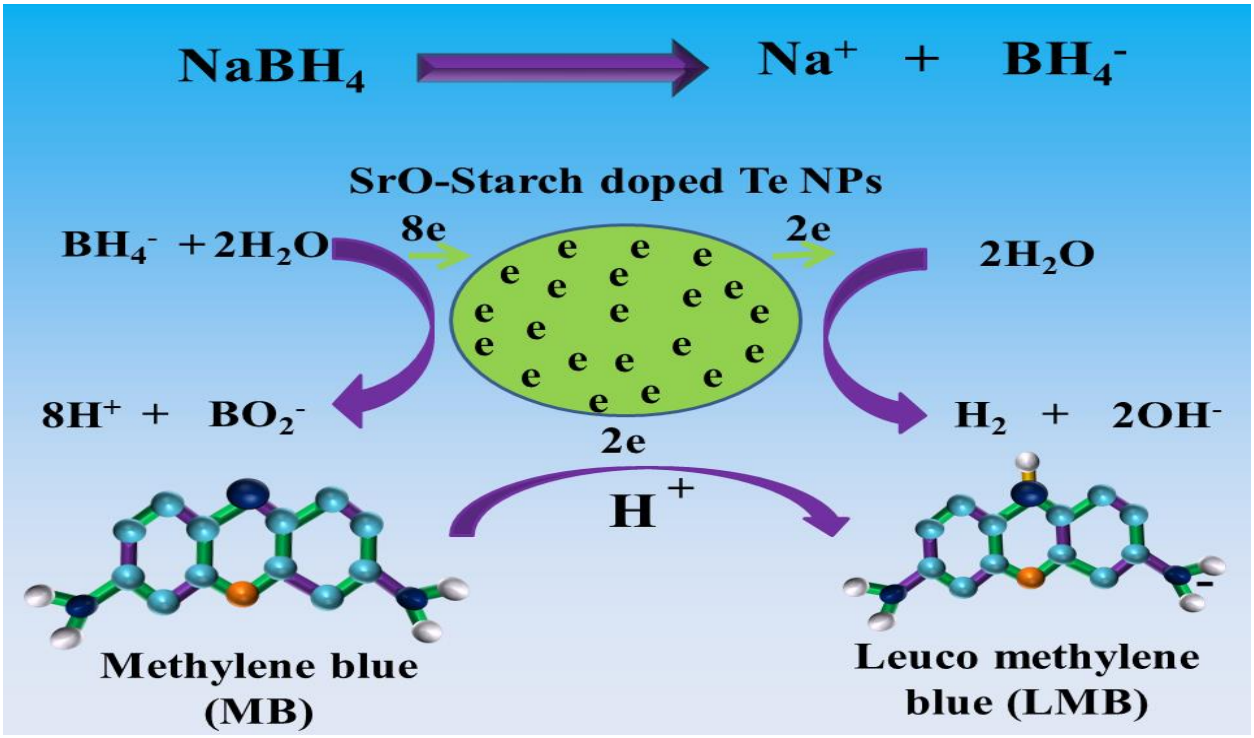

Fig. 2 Schematic description of catalytic performance

2.4 Isolation and identification of *S. aureus* and *E. coli*

Samples of caprine mastitic (bovine milk) have all been obtained from various farmlands in Punjab, Pakistan. These samples have been cultivated on 5% blood sheep agar. The cultivated specimens were preserved at 37 °C for 24 hours, swabbed on manitol salt agar (MSA) and MacConkey agar (MA) to separate purification of *Escherichia coli (E. coli)* and *Staphylococcus aureus (S. aureus)* correspondingly. Morphological analysis, Gram staining, and biochemical tests have been used to classify extracted colonies through catalase and coagulase tests.

2.5 Antimicrobial activity

The agar well diffusion approach was used to investigate the antibacterial activities of as-synthesized samples against Gram +ve and Gram –ve pathogens [22]. Bacterial strains have been

preserved in nutrient agar plates. The activated growth of bacterial strains on MA and MSA has been swabbed over Nutrient broth with 0.5 McFarland standard (1.5 108 CFU/mL) against *E. coli* (G -ve) and *S. aureus* (G +ve). The wells with a 6 mm diameter of approximately have been developed by applying a sterile cork bore, and SrO, SrO-starch composite, and Te doped SrO-starch composite at low and high concentrations (0.5 mg/50 µL) and (1.0 mg/50 µL), respectively, have been encumbered through each well, with ciprofloxacin and DI water (0.005 mg/50 µL) and (50 µL) going to serve as +ve and −ve controls, correspondingly. After incubating the synthesized samples at 37 °C for 24 hours, the antimicrobial potential was used to calculate the inhibition zone (mm) measurement with the help of a Vernier caliper. Antimicrobial efficiency was calculated statically by measuring the zone (mm) of inhibition by applying an ANOVA (one-way analysis of variance) [23].

2.6. Molecular Docking Studies

Nanoparticles have been extensively studied for various biological applications, particularly drug delivery, bio-sensing, bio-imaging and antibacterial agents. The biological potential of metal nanoparticles depends on their well-characterized composition, size, crystallinity and morphology [24]. The use of computational techniques to clearly understand the mechanism behind given bioactivity has recently gained much attention. Here, we performed molecular docking studies of SrO-starch and Te/ SrO-starch nanocomposites against selected enzyme targets, i.e., *β*-lactamase and DNA gyrase from *E.coli*. Because *β*-lactamase and DNA gyrase are essential for bacterial survival as they facilitate cell wall synthesis and nucleic acid synthesis, we selected them as possible targets [25,26].

Crystal structures of β-lactamase$_{E.coli}$ and DNA gyrase$_{E.coli}$ were retrieved from protein data bank having accession codes 4KZ9 (Res: 1.72 Å) [27] and 5MMN (Res: 1.90 Å) [28], respectively. Molecular docking predictions were performed using ICM version 3.8-7d (Molsoft L.L.C., La Jolla, CA) [29]. Protein structure preparation was done using the receptor preparation tool of ICM software, where key steps involved were energy minimization (using default force field), addition of H-atoms and gastegier charges, removal of native ligand and H_2O molecules. The binding pocket was specified around co-crystallized ligand, i.e., within 5 Å vicinity using a grid box. Finally, best-docked conformations generated in each case were selected and analyzed further.

The unit cell (monomer structure) of nanocomposites were prepared using ligEdit tool of ICM and lowest energy/stable conformation was generated in each case and later optimized. The docked complexes were analyzed using Discovery studio visualizer and Pymol software to generate a 3D-view of binding interactions within the active pocket.

3. RESULTS AND DISCUSSION

The crystal patterns, phase composition and crystalline size of pristine, SrO-starch composite and Te-doped SrO-starch composite NPs were investigated and identified using XRD (Fig. 3a). Characteristics peaks of diffraction at angles of 25.5°, 29.9°, 32.9°, and 49.9° have been appointed to the planes (110), (111), (011), and (220) cubic SrO space group Fm-3 m and space group number 225 (JCPDS 00-006-0520) and matched with DB card number 1011328. Additional, the diffraction peaks at 35.59° and 75.3° were assigned to the (110) and (220) planes of tetragonal SrO_2 with space group numbers 139 and with space group 14/mmm well-matched with JCPDS 00-001-1113. In addition, the peaks of diffraction have been observed at 2θ

values 39.2°, 43.2°, 46.3°, 54°, 57.3°, 62.9°, 66.2°and 68.5° correspond to the planes (410), (401) (400), (511), (210), (322), (141) and (241) of strontium hydroxide $Sr(OH)_2$ with the JCPDS card No. 71-2365 and matched with DB card number 9008161 indicating the existence of $Sr(OH)_2$ in the synthesized samples respectively. The sharp peaks indicated the formation of high crystalline powders for SrO and $Sr(OH)_2$. Amylose and amylopectin have been recognized as the significant elements of starch, representing the crystalline and amorphous phases as a result, starch is a semicrystalline material. The amylose yields the starch's crystalline region with a linear structure, while the amylopectin generates the starch's amorphous phase with a branched structure [30–32]. The starch spectrum has a broadband region of 10° and 27° with distinct peaks. The starch XRD spectrum indicates two strong diffraction peaks at 12.9° and 19.7° [33]. Due to the low relative amount of starch-doping concentration, no predominant peaks of starch emerged in doped samples. The SrO-starch composite causes the sharp peaks in the graph to shift. With 2% Te doping in SrO-starch composite, the peak intensity of the sample increased; as the concentration of doping increased, the intensity increased, and the bandwidth decreased. The purity and crystallinity have been indicated by the strong and sharp peaks of the samples. The main reason for the crystals disposition of nanocomposites materials for the structure of metal–oxygen, strongly influenced by a wide range of restrictions such as time, reaction temperature and fabrication process [34]. The crystalline size of prepared nanopartical can be calculated from the most intense peak of all prepared samples using the Debye–Scherrer formula was 26.18 nm, 10.5 nm, 8.22 nm, and 5.98 nm with corresponding plane (110) and (011) for SrO and, SrO-starch composite and Te (2, 4%) doped SrO-starch composite, respectively.

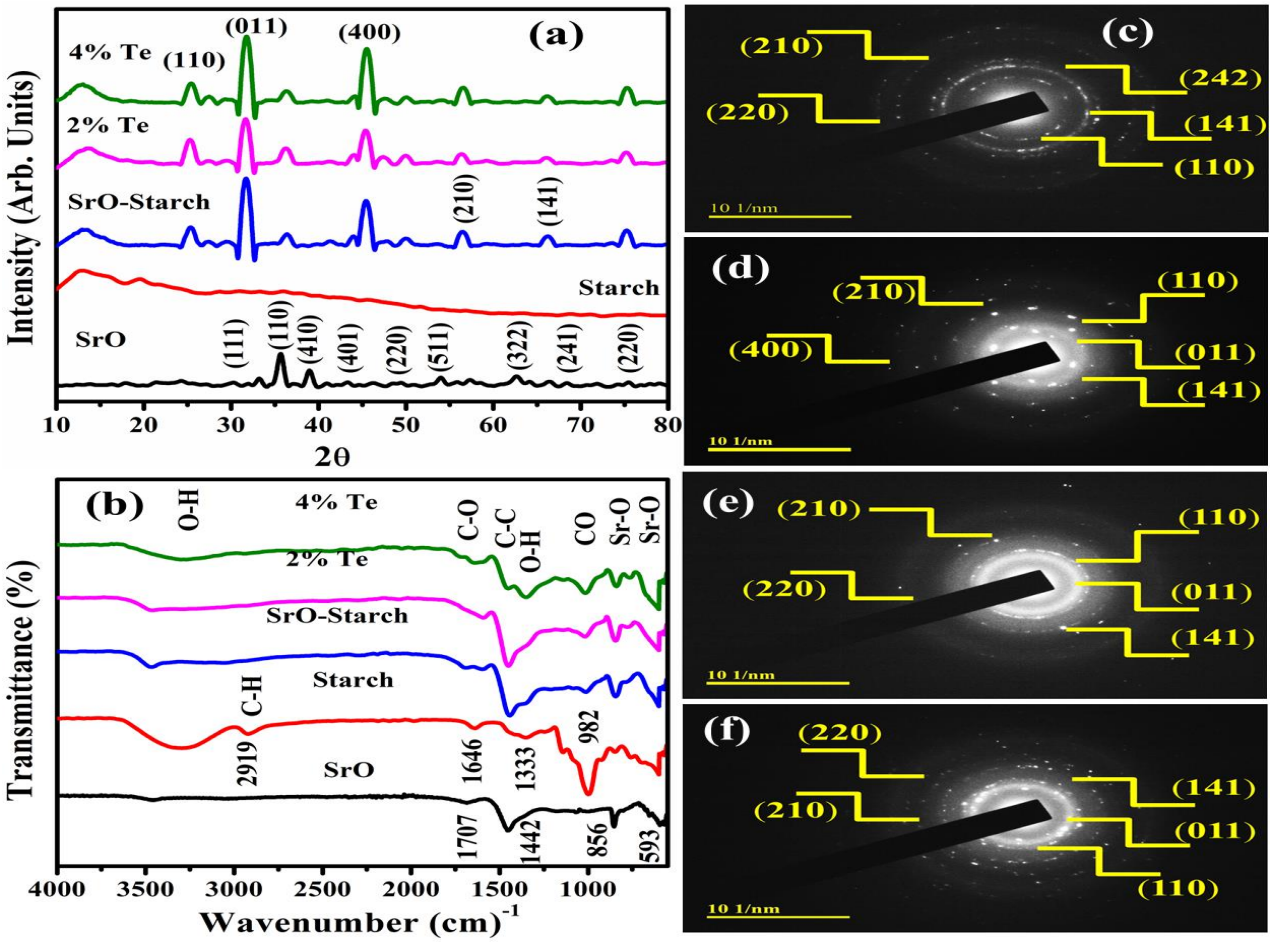

Fig. 3 (a) XRD pattern prepared NPs (b) FTIR spectra (c) SAED pattern of SrO NPs, (d) SAED pattern of SrO-starch composite (d) SAED pattern of 2% Te doped composite NPs, (e) SAED pattern of 4% Te doped composite NPs.

FTIR spectra of prepared NPs have been analyzed in the range of 4000-400 cm^{-1} to clarify the chemical functional groups in specimens indicated in (Fig. 3b). The FTIR spectra of SrO NPs have bands between 500 and 1000 cm^{-1} at 592 cm^{-1} ascribed to Sr–O stretching, and bond at 856.39 cm^{-1} assigned to Sr-O bending vibrations confirming the SrO formation. The effectiveness of these bands is strongly dependent on the reaction conditions, and at high temperatures, a strong Sr–O–Sr molecular structure has been established [34]. The C–C bonding

and C–O stretching vibration of bonds are responsible for the bands observed near 1707 and 1442 cm^{-1}, correspondingly [10]. The FTIR spectrum of starch revealed broadband near at 3298, 2923, 1646, 1333, 1240, 1157, and 982cm^{-1}. The strong band at 3298 cm^{-1} was associated with starch O–H stretching bond, and its width has been credited to intermolecular and intramolecular hydrogen bond formation. The observed band at 2919 cm^{-1} has asymmetric C–H stretching characteristics. The observed band at 1157 and 982 cm^{-1} assigned to CO and CC stretching with contributions of COH [35]. The bands appeared at 1240 cm^{-1} and 1333 cm^{-1} have been used to ascribe the O-H bending of alcohols (primary or secondary). Because of the hydrophilic nature of starch, a single peak has been detected at approximately 1646 cm^{-1}, which is associated with a water (H_2O) molecule tightly bound with starch [36,37]. Starch has two populations of water: one of them is hydrogen bonding in the crystalline structure of starch and the other is hydration of water considered water freer [38]. Starch strongly interacts with water molecules in both amorphous and crystalline structures, affirming by the FTIR spectrum [39]. In SrO-starch composites, the broadband was obtained at 842, 1014, 1350, 1440, 1592, 1688, and 3468 cm^{-1}, which shows increasing bandwidth and indicates the band transformation caused by a reduction in atomic order arrangement within the unit cell structure. Te atoms are distributed uniformly on the surface of SrO which adsorbs oxygen and prevents SrO aggregation, decreasing bond intensity. As indicated by increased intensity transmission, the coupling effect is more pronounced in Te–SrO than in starch–SrO. This could have been assigned to a non-significant increment in the length of bond separation as the consequence of composite doping [40]. SAED has been utilized to identify polycrystalline and single-crystalline structures in nature and show that the structure is amorphous. Electron diffraction profiles obtained from SAED rings were indicated in Fig.3 (c-f). SAED has been implemented to recognize crystal structures

apparent from the diffraction rings that are in a circular shape and indicate the polycrystalline nature of the synthesized materials. With increasing the concentration of Te in SrO-strach composite, crystallinity increases. The Obtained rings are highly crystalline and well-matched with the results of XRD.

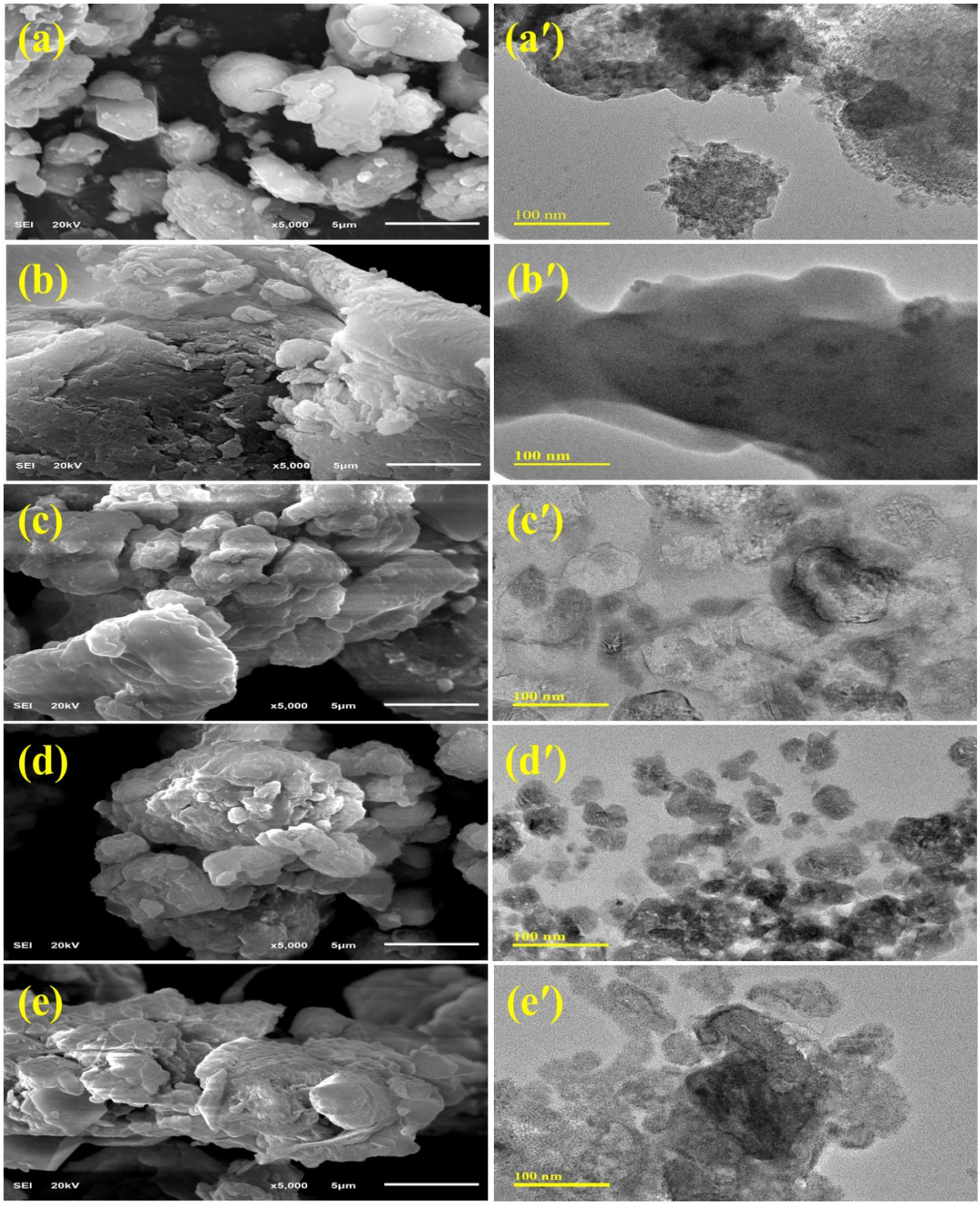
(a)
SEI 20kV x5,000 5μm
(a′)
100 nm
(b)
SEI 20kV x5,000 5μm
(b′)
100 nm
(c)
SEI 20kV x5,000 5μm
(c′)
100 nm
(d)
SEI 20kV x5,000 5μm
(d′)
100 nm
(e)
SEI 20kV x5,000 5μm
(e′)
100 nm

262

Fig. 4 a–e SEM micrographs and a′-e′ TEM micrograph of a) SrO, b) starch, c) SrO-starch composite d) 2% Te doped SrO-starch composite, and e) 4% Te doped SrO-starch composite nanoparticles.

The structural and surface morphology of synthesized NPs has been examined through FE-SEM, TEM and HR-TEM, as revealed in Fig.4.The SEM morphology confirms the particles are agglomerated as represented in Fig 4 (a′-e′) in a composite. The agglomeration increasedand chunks like morphology were obtained by incorporating Te into the composite. In TEM images, the pristine sample was aggregated with SrO NPs, indicating agglomeration of particles. The nanoparticle of starch shows a smooth surface and layer-like properties as the polymer mostly make the layer-like structure represented in Fig. 4b and 4b′. Upon doping starch in SrO, the nanoparticle can be seen clearly with small size, as indicated in Fig. 4c. Further, Te (2 %) doping into the composite resulted in the aggregation of nanocomposites that were distributed randomly over the starch surface. Figures 4d, e indicate the existence of NPs with aggregated dopants. The configuration of a triplex composite (Te/SrO–starch) network in the shape of NPs has been confirmed by increasing the doping concentration of Te into SrO-starch composite, as shown in Fig. 4e, a higher concentration of Te (4%) has been noticed. The triplex structure may improve charge carrier separation and transportation (electron and holes) as a consequence of improving the catalytic degradation of dye.

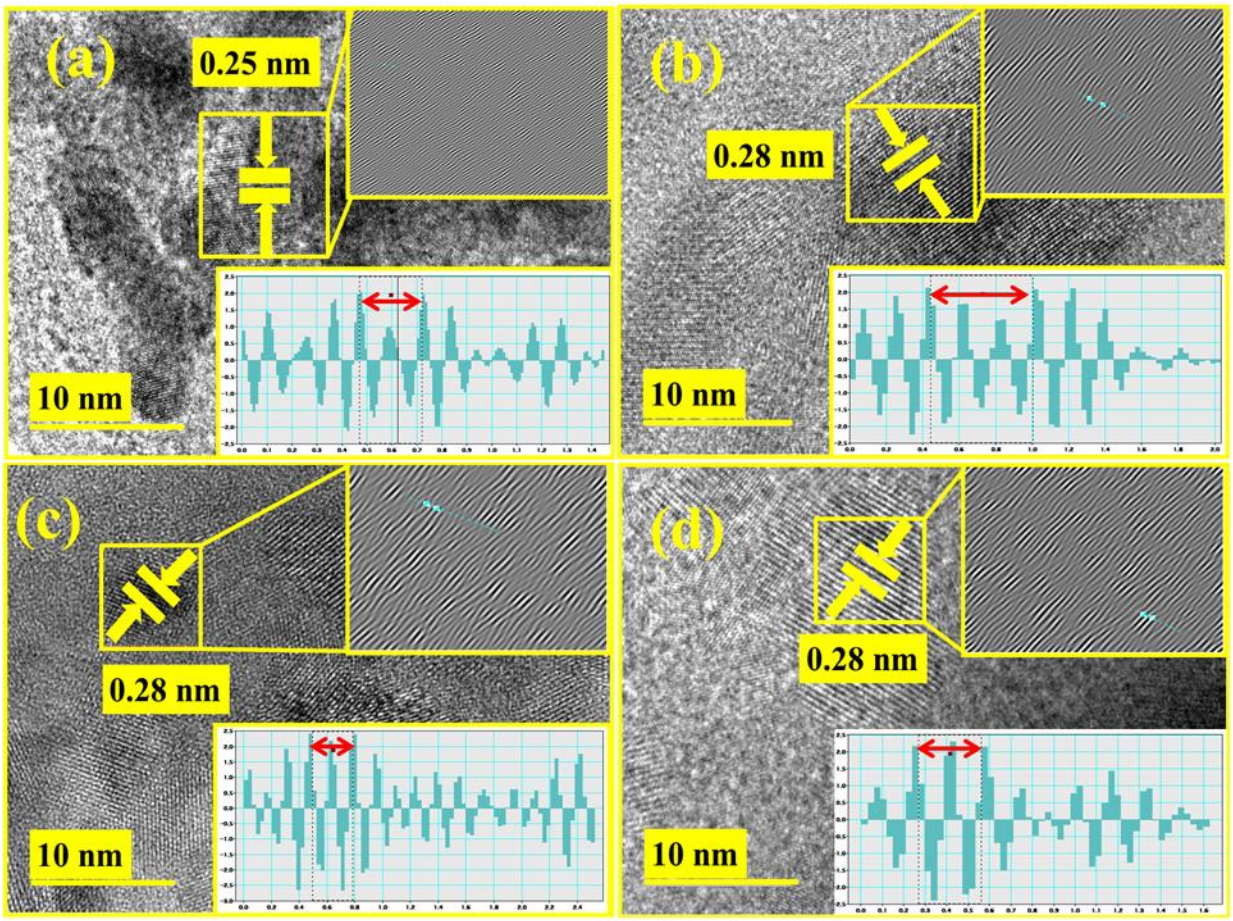

Fig. 5 Calculated interlayer d-spacing using the HR-TEM micrograph of a) SrO, b) SrO-starch, c) Te (2 %), and d) Te (4 %) samples.

HR-TEM micrograph has been used to measure the interlayer d-spacing measurements of pristine, SrO-starch composite and composites doped samples calculated throughout Gatan digital-micrograph software using IFFT and FFT. HR-TEM pictures are used to make a distinction lattice fringes. The measured interlayer spacing of samples is represented in Fig.5 (a-d). The measured d-spacing value of pristine SrO NPs is 0.25 nm, corresponding to (110) plane. The SrO-starch composite and Te (2 and 4%) doped composite have a d spacing value of 0.28 nm corresponding to the plane (011).

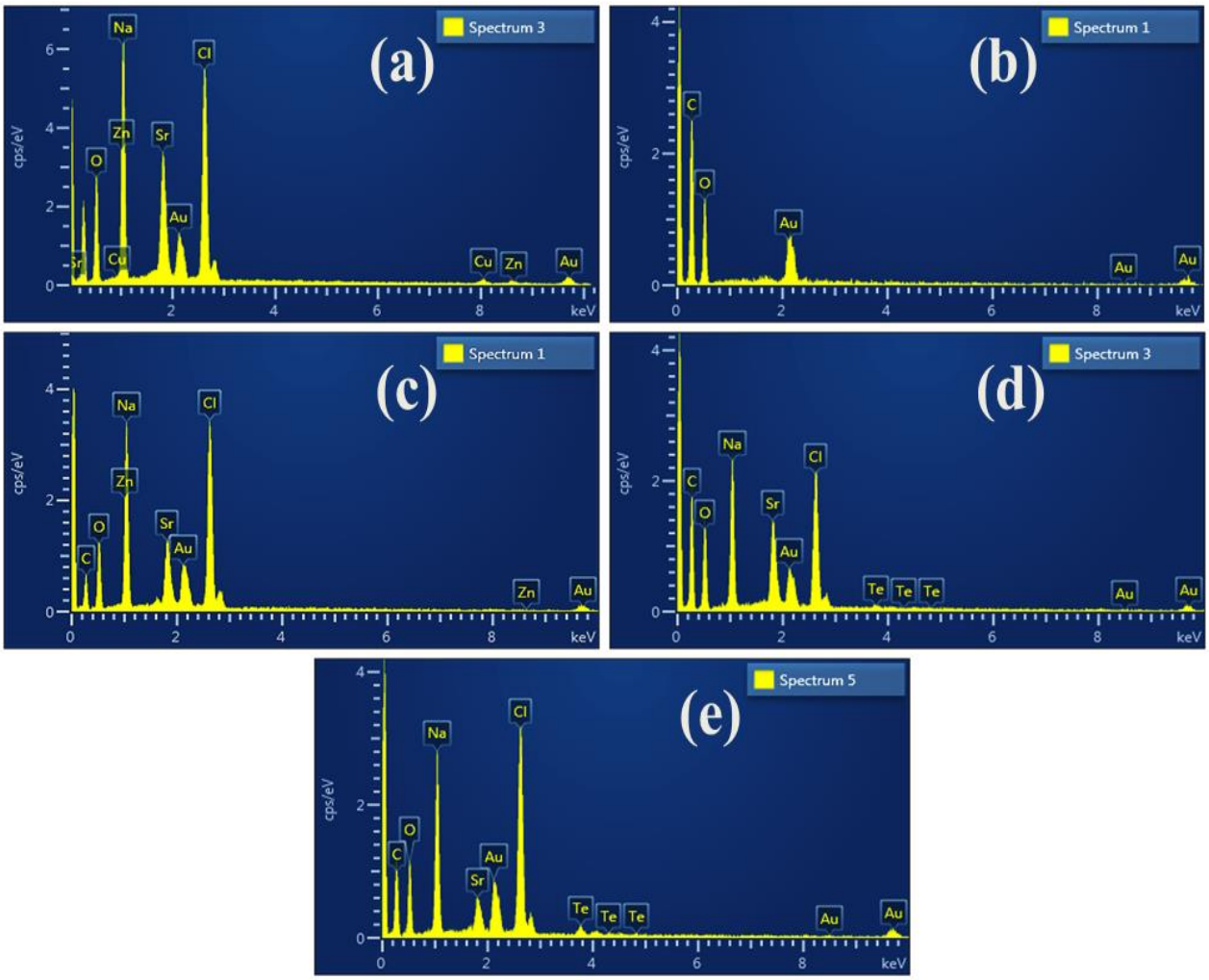

Fig. 6 EDS analysis of SrO, SrO-starch composites (a–e) with Te doped content (2 and 4 %).

Electron diffraction spectroscopy (EDS) has been used to investigate the stoichiometric analysis and composition of pure SrO, starch, starch-SrO composite, and co-doped samples indicated in Fig. 6. The obtained EDS profile pictures exhibit different peaks for SrO, as shown in Fig 6a. Cl signals in EDS spectra may be interpreted as an impurity picked up during sample preparation. Copper (Cu) is extensively used in detectors an artificial Cu peak was observed in spectra. The Cu signal could also arrive from the stubs that have been components of the specimen holder

used throughout the EDS analysis [41]. Small peaks of sodium (Na) have been appeared because NaOH used to regulate the pH of the prepared solution. In Fig. 6b, the peaks of carbon and oxygen show successful starch synthesis. Fig .6c revealed the preparation of starch-SrO composite, and Fig. 6d and e show successful doping of Te into the composite.

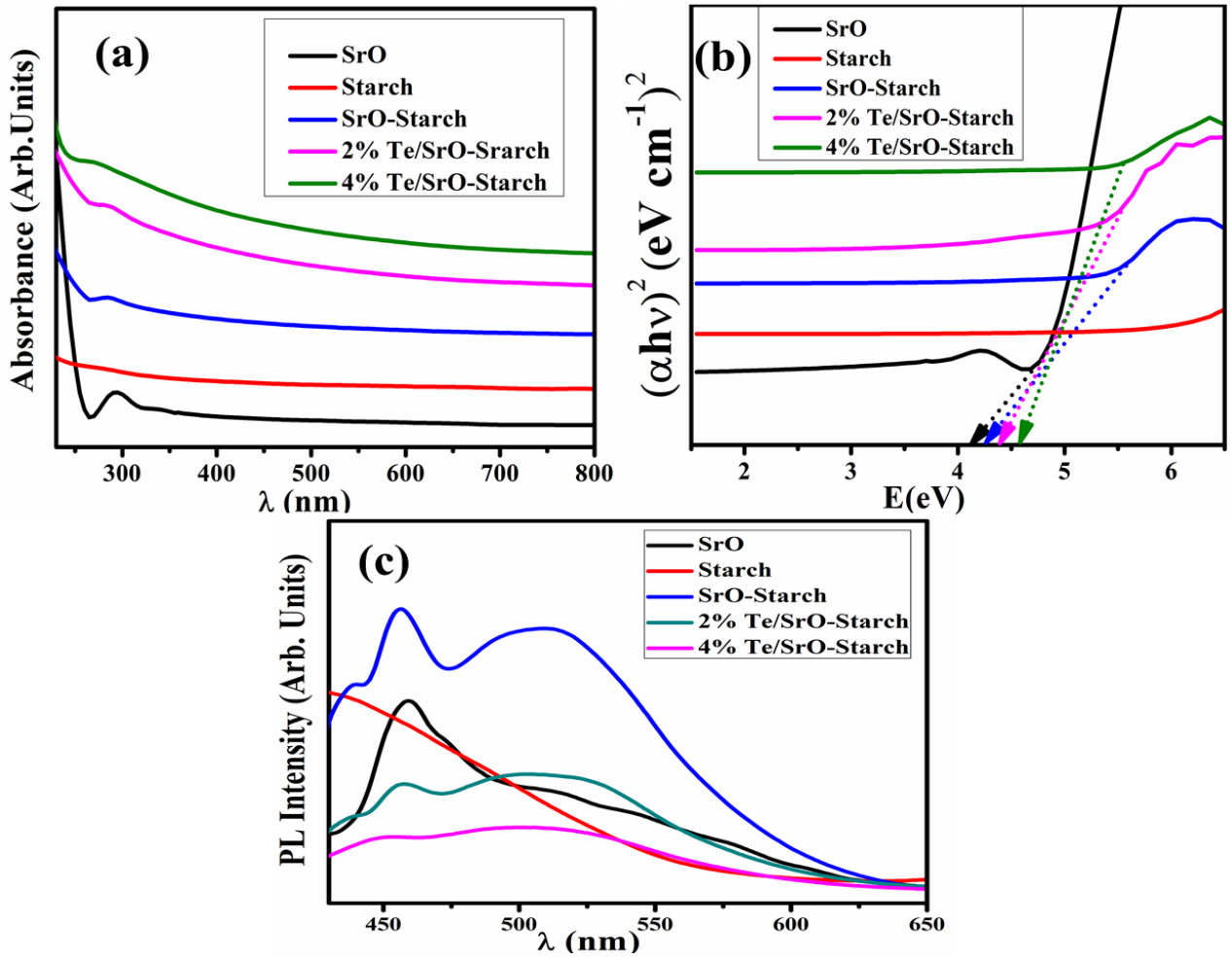

Fig. 7 a) Absorption UV–Vis spectra, b) Tauc plot energy band gap, and c) PL emission spectra of synthesized nanoparticles

UV–Vis spectra have been used to examine the range of 200–800 nm for optical evaluation of prepared Te/SrO–starch NPs (Fig.7 a). The absorption band in the spectra has been

demonstrated at 293 nm, 250, and 270–287 nm for SrO, starch, and composites, as well as co-doped SrO-starch composites with Te (2 and 4%), indicating the purity and controlled size of the particles. The excitonic absorption of SrO at 293 nm reflects quantum size effects caused by the formation of monodispersed nanoparticles [34]. After Te (2 and 4%) doping in a composite (SrO-starch), a blue shift was observed. This represents that the crystalline size decreased, asindicated in XRD analysis. The energy bandgap (Eg) of synthesized samples was determined by extrapolating the linear portion using the Tauc plot by $(hv)^2$ vs hv represented in Fig.7b. The Eg of the control SrO sample was 4.23 eV, whereas co-doping of starch and Te in the lattice resulted in an increase in energy band gas of up to 4.59 eV. SrO NPs have a band gap energy of 4.23 eV higher than bulk SrO. The trend of decreasing particle size influences the increase in the energy bandgap of the synthesized sample owing to the effect of quantum confinement. The increased Eg result represents that the prepared SrO NPs in this work are in nanophase.

Photoluminescence (PL) has been used to investigate the charge carrier (e^-, h^+) trapping and charge carrier transfer efficiency, as well as to comprehend the rate of recombination of electron hole-pair [42]. PL emission spectra of pristine SrO, composite, and Te doped composites have been retrieved at an excitation wavelength λexc=350 nm depicted in Fig. 7c in the range of 400-700 nm to investigate the transfer and recombination rate of charges. Pure SrO exhibited a broadband emission in the 450–460 nm range, which is consistent with the range expected by Nemade and Waghuley, who affirmed the SrO emission spectrum of quantum dots synthesized via chemical precipitation in the range of 320–500 nm [43]. Energy gap values have been transformed by size and surface composition variations, which were suggested to affect the range of emission frequency. Differences in the size of particles, energy band gap values and surface morphology account for the minor difference between the current outcomes and those

observed by Nemade and Waghuley. It has been expected that the PL with lower emission intensity correlates with a lower rate of charge carrier of electron and hole recombination [44]. Starch demonstrated the PL emission peak at 413 nm and raised PL emission intensity, denoting that transfer rates increased after starch was doped in SrO to generate the synthesized composite. Composite doped with Te (2 %) concentration increased the transfer rate; however, increasing the concentration of Te (4 %) doped composite resulted in a decrease in PL intensity. This decrease in PL intensity after Te incorporation in composites demonstrates that recombination of charges has been suppressed in the composite, which is very beneficial for superior catalytic activity and antimicrobial actions.

CA of synthesized samples has been examined to determine the % dye degradation efficiency against MB in the existence of $NaBH_4$ in acidic, neutral, and basic media Fig.8. The catalytic dye degradation has been highly dependent on the solution pH, the adsorption characteristics of the nanocatalyst, the shape and surface area of the catalyst, crystallinity, and morphology of the nanomaterials [45,46]. CA is influenced by the diffusion of dye molecules and reducing agents on the surface catalyst, adsorption on the surface, oxidation and reduction reaction, decomposition of resultant species, and product diffusion apart from the surface of the catalyst, as represented in Fig. 2. The catalyst plays an essential function between the dye and the reducing agent, an electron relay, increasing the rate of oxidation and reduction on the catalyst's surface [47]. The small size particles provide a large surface area which is beneficial for dye degradation. According to the results of an XRD study, as the concentration of Te increases to the optimal level, the particle size decreases. This leads to a higher surface area, resulting in a high catalytic activity on the MB dye degradation.

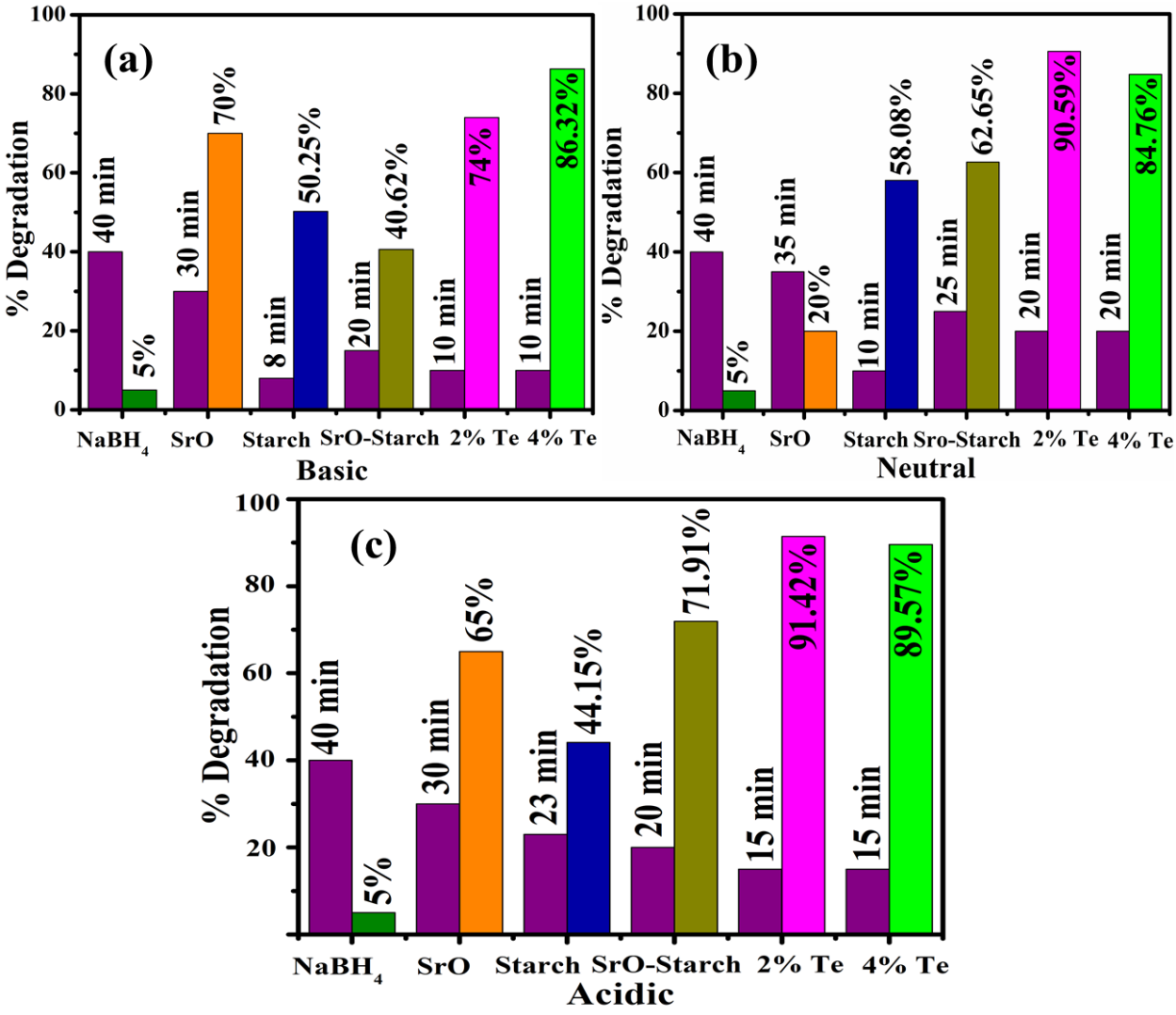

354

355 **Fig. 8** Catalytic dye degradation activity of synthesized samples in a) basic, b) neutral, and c)

356 acidic medium.

357 According to the experimental results, the maximum degradation of dye was noticed in both

358 basic and acidic media, as represented in Fig.8 (a-c). A 3 mL MB solution has been marked as

359 the targeted dye for the investigation. A reducing agent NaBH4 (200 µL) was then incorporated

360 into the prepared dye solution. The reducing agent decided to act as an electron carrier for the

361 dye molecule, causing them to degrade. After incorporation of reducing agent, only 5 % of dye

362 has been observed to degrade. This is mainly attributable to $NaBH_4$ acting as an electron relay to

transfer electrons and lower catalytic activity without any catalyst to degrade the dye molecule. The synthesized nanocatalyst (400 μL) has been accumulated into the solution, leading to an improvement in the degradation of dye and considerable catalytic performance, approximately 91.42 % dye in 20 minutes in an acidic medium. Furthermore, the entire performance was carried out at 25 ºC. The samples have been spectrophotometrically examined in the 200–800 nm range.

The pH value is critical throughout the catalytic activity. Furthermore, pH plays a significant role in textile effluents, and the molecular mechanism includes dye degradation. It is significant to mention that the % degradation of dye is directly proportional to the pH value. At neutral pH the pure SrO indicated 20% degradation of dye in 35 min and starch revealed 58% degradation of dye in 10 min. The SrO-starch composite demonstrated dye degradation of 62.65% in 25 min. Upon further doping, 2% Te shows 90% and 4% Te indicates 84.76% dye degradation in 20 min.

NaOH solution has been utilized to sustain the dye for the basic medium at pH ~ 12, as represented in Fig. 8a. Pristine SrO degrades the dye solution by 70% in 30 minutes, and starch indicates 50.25% degradation in 8 minutes. The composite of SrO-starch presented dye degradation of 40.62% in a time of 20 min. Te (2 %) degradation of dye 74% of MB in basic medium. Te (4 %) sample exhibited dye degradation of MB 86.32% in 18 min. Although there is a scarcity of H^+ atoms in basic medium, the excess of hydroxyl (OH^-) ions comes from NaOH adhere to the catalyst surface and induce a net negative charge on the catalyst surface. The positively charged surface (cationic) of MB dyes in nature attracts the negatively charged surface of catalyst as the consequence of adsorption has been accomplished. As previously stated, CA depends on the adsorption capacities of the catalyst surface, so adsorption increased in basic medium encourages significant interaction against MB and the catalyst surface that are positively and negatively charged surfaces, respectively, resulting in high efficiency of

386 dye degradation [48]. For acidic medium Fig. 8c, H_2SO_4 has been used to maintain the pH ~3 of
387 dye solution. Pristine SrO revealed a maximum degradation of 65% in 30 min of dye, and starch
388 indicated a dye degradation of 44.15% in 23 min. The composite of SrO-starch indicates dye
389 degradation of 71.91% in 20 min, and the co-doped sample revealed 91.42% for 2% Te doping
390 and 89.57% for 4% Te doping in time for 15 min, respectively. The degradation of MB
391 dye occurs through the degradation process, in which it receives electrons generated from $NaBH_4$
392 (reducing agent) through a catalyst surface. The existence of H_2SO_4, which contributes to the
393 reduction of MB into leuco-methylene blue (LMB), is the cause of enhanced CA in acidic
394 conditions. The nanocatalyst can transfer electrons from $NaBH_4$ to the MB dye and electrons
395 from $NaBH_4$ to the MB dye, resulting in the reduction of dye molecules [48]. The 4%-Te/SrO-
396 starch sample revealed higher dye degradation in acidic, basic, and neutral mediums. The 2% -
397 Te/SrO-starch catalyst demonstrated excellent catalytic activity in an acidic medium, serving as a
398 superior catalyst for maximum dye degradation. According to experimental results, the highest
399 dye degradation value was observed in acidic conditions.

400 **Table 1**: Antibacterial activity of SrO, SrO-starch composite, and Te (2 and 4%)/SrO-starch for
401 Gram-positive and negative bacteria strain

Samples	*S. aureus*		*E. coli*	
	Inhibition zone (mm)		Inhibition zone (mm)	
	0.5 mg/50 µL	1.0 mg/50 µL	0.5 mg/50 µL	1.0 mg/50 µL
SrO	0	0.95	0	0.9
SrO-starch	1.25	3.15	0	1.8

2% Te/SrO-starch	2.20	6.25	1.85	2.55
4% Te/SrO-starch	3.10	9.30	2.30	3.25
Ciprofloxacin	9.20	9.20	4.25	4.25
DI water	0	0	0	0

402

403 In vitro antimicrobial activity of the SrO, SrO–starch and Te doped SrO–starch composite
404 nanoparticles for G −ve and G +ve bacteria has been investigated by calculating the inhibition
405 zone, applying the agar method well diffusion represented in Table 1. The extracted data indicate
406 enhancement in bactericidal potential in comparing both *S. aureus* and *E. coli* bacteria. Pristine
407 SrO, SrO-starch composite, and Te doped SrO-starch composite NPs samples revealed
408 enhancement in antimicrobial activity against *S. aureus* in the comparison of *E. coli* bacteria.
409 Substantial zones (nm) of inhibition for *S. aureus* and *E. coli* for bactericidal potential for
410 pristine simple were calculated as (0–0.95 mm) and (0–0.9 mm), including both for G +ve and G
411 −ve at lower and higher concentration. SrO–starch composite effectively improved the
412 bactericidal potential represented by the inhibition zones measurement at high and low doses has
413 been recorded as (1.25–3.15 mm) and (0–1.8 mm) between *S. aureus* and *E. coli*
414 correspondingly. Te doped SrO–starch composite nanoparticle effectively improved the
415 bactericidal potential on G +ve compared with G –ve bacterial strains. 2% Te doping in the
416 composite represents the inhibition zones (mm) measurements that have been recorded as (2.20–
417 6.35 mm) and (1.85–2.55 nm) at high and low doses toward *S. aureus* and *E. coli*,
418 correspondingly. At 4% doping in the composites, the inhibition zone measurements for *S.*
419 *aureus* and *E. coli* at low and high doses were represented (3.10–9.30 mm) and (2.30–3.25 mm),

respectively. Ciprofloxacin has been utilized as the positive control presented (9.20 mm) and (4.25 mm) inhibition zones against *S. aureus* and *E. coli*, correspondingly in comparison with DI (0 mm) water used as a negative control. Ultimately, the Te-doped composite NPs indicate outperformed antimicrobial efficiency between G +ve contrast to the G –ve bacterial strain. Gram-positive bacteria have a cell wall typically containing a thin layer of peptidoglycan, teichoic acid, and numerous pores. These pores allow foreign molecules to infiltrate the cell wall, which causes damage to the cell membrane and ultimately results in cell death. Additionally, compared to Gram-negative bacteria, Gram-positive bacteria have a strong negative charge on the cell wall surface, which can attract NPs.

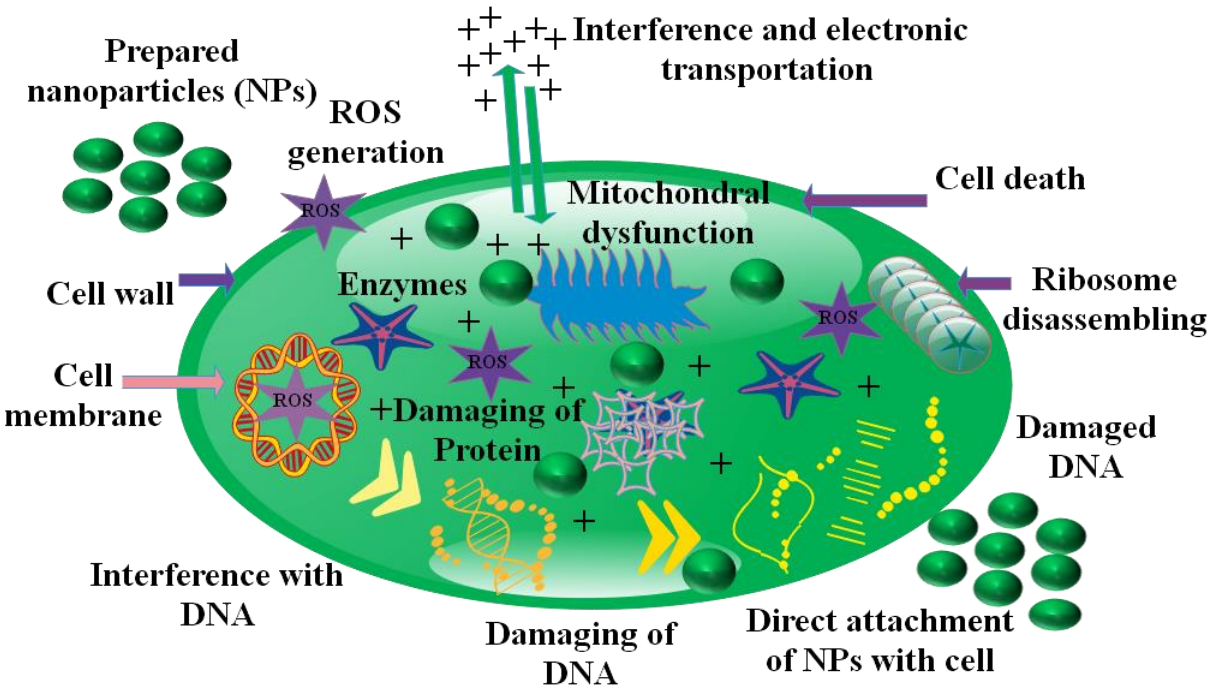

Fig. 9 Schematic description of antimicrobial activity.

The synthesized SrO and Te doped SrO–starch composites NPs generate reactive oxygen species (ROS) in the presence of light during incubation, as represented in Fig. 9. The oxidative stress

tolerance has been determined by particle size, morphology and surface area of prepared nanomaterials, small size NPs having large surface area all of which play a role in antimicrobial action potential [49,50]. The electron-hole pairs serve as the primary unit for generating reactive oxygen species (ROS). The chemical process includes the production of enhanced levels of reactive oxygen species (ROS) such as superoxide anion radical ($*O^{-2}$), hydroxyl radical ($*OH$) and hydrogen peroxide radicals($*H_2O_2$). Many transition metal oxides are sportive against microorganisms due to the interaction of hydrophobic and electrostatic forces. The production of reactive oxygen species (ROS) can be explained as follows [51–53].

$$SrO + h\nu\ (photon) \rightarrow h^+\ (hole) + e^-\ (excited\ electron)$$

$$e^-\ (excited\ electron) + O_2\ (surface\ oxygen\ molecule) \rightarrow *O_2^-\ (superoxide\ anion\ radical)$$

$$h^+\ (hole) + H_2O\ (water\ molecule) \rightarrow OH^- + H^+$$

$$*O^-_2\ (superoxide\ anion\ radical) + H^+ \rightarrow *HO_2\ (hydroperoxyl\ radical)$$

$$*HO_2\ (hydroperoxyl\ radical) + e^-\ (excited\ electron) + H^+ \rightarrow *H_2O_2\ (hydrogen\ peroxide)$$

$$*H_2O_2\ (hydrogen\ peroxide\ radical) + *O^-_2\ (superoxide\ anion\ radical) \rightarrow *OH\ (hydroxyl\ radical) + O_2\ (singlet\ oxygen) + OH^-\ (hydroxyl\ ion)$$

Sro, Sro-starch and Te-incorporated Sro-starch are exposed to light with the energy of photon equal to the energy bandgap of semiconductor and electrons from the valence band (VB) are transferred to the conduction band (CB), leaving holes in the valence band. These excited electrons (e^-) in the CB can be trapped by the oxygen molecules (O_2) present on the surface, producing superoxide anion radicals. Similarly, the holes in the VB react with the water molecules (H_2O), emitting hydroxyl and hydrogen ion. The superoxide anion radicals (O^-_2)

interact with H^+ ions to produce hydroperoxyl radical ($*HO_2$). The hydroperoxyl radical ($*HO_2$) combines with e^- and H^+ resulting in hydrogen peroxide radical ($*H_2O_2$). At the same time, hydrogen peroxide radical ($*H_2O_2$) can react with superoxide anion radicals ($*O^-_2$) to generate hydroxyl radical ($*OH$), hydroxyl ion (OH^-) and singlet oxygen (O_2). Negatively charged radicals (hydroxyl radicals and superoxide anions) cannot penetrate microorganism cell membranes, but they can cause critical damage to the bacteria's outer surface, whereas positively charged hydrogen peroxide radicals ($*H_2O_2$) can easily penetrate negatively charged bacterial cell membranes and kill the bacteria. Therefore, hydrogen peroxide radical ($*H_2O_2$) is highly harmful to damaging the bacterial cell membranes and causes the death of bacteria.

The electrostatic interaction among both bacterial strains and composites nanomaterials generates ROS that attaches to the bacterial cell membrane, resulting in the extrusion of cytoplasmic content and structure and the annihilation of bacteria present to be willing to take responsibility for bacterial cell death [54–58]. The anti-bacterial efficiency of NPs is reversed as their size increases [23,49,55]. Two reactions for nanomaterial response with the strains of bacteria have been discovered, including electrostatic interactions of cations (Sr^{+2} and Te^{+2}) with the bacterial cell that is negatively charged as a result of the collapse of micro pathogenic organisms [56,59,60].

The biological activities of nanomaterials are well-documented. They may interact with bacterial cells disrupting cell membrane permeation and destroying key metabolic pathways. Still, the exact mechanism behind nanoparticle toxicity toward bacteria is unknown [61,62]. Computational methods have been extensively employed during the last few decades to analyze various forces behind bioactivity of interest. Enzymes belonging to pathways essential for

476 bacterial growth and survival have been considered attractive targets for discovering new drug
477 leads [63].

478 β-lactamase$_{E.coli}$ has previously been reported as an attractive target for antibiotics discovery
479 [64]. Here, we evaluated the binding tendency of SrO-starch and Te/ SrO-starch nanocomposites
480 inside the active pocket of β-lactamase$_{E.coli}$. The best-docked conformation observed for SrO-
481 starch revealed H-bond interaction with Glu245 (2.4 Å), Asn244 (1.8 Å), Pro181 (2.2 Å),
482 Arg232 (1.9 Å) with overall binding score -10.792 kcal/mol. Te/ SrO-starch nanocomposite also
483 showed H-bonding interaction with Asp242 (2.1 Å), Asn244 (2.0 Å), Arg232 (2.7 and 1.7 Å),
484 and Pro181 (2.5 Å) alongside C-H interaction with Ile243 and Pro181. The binding score for Te/
485 SrO-starch nanocomposite with β-lactamase$_{E.coli}$ was -11.658 kcal/mol. The binding interactions
486 of both synthesized nanocomposites are shown in Fig. 10.

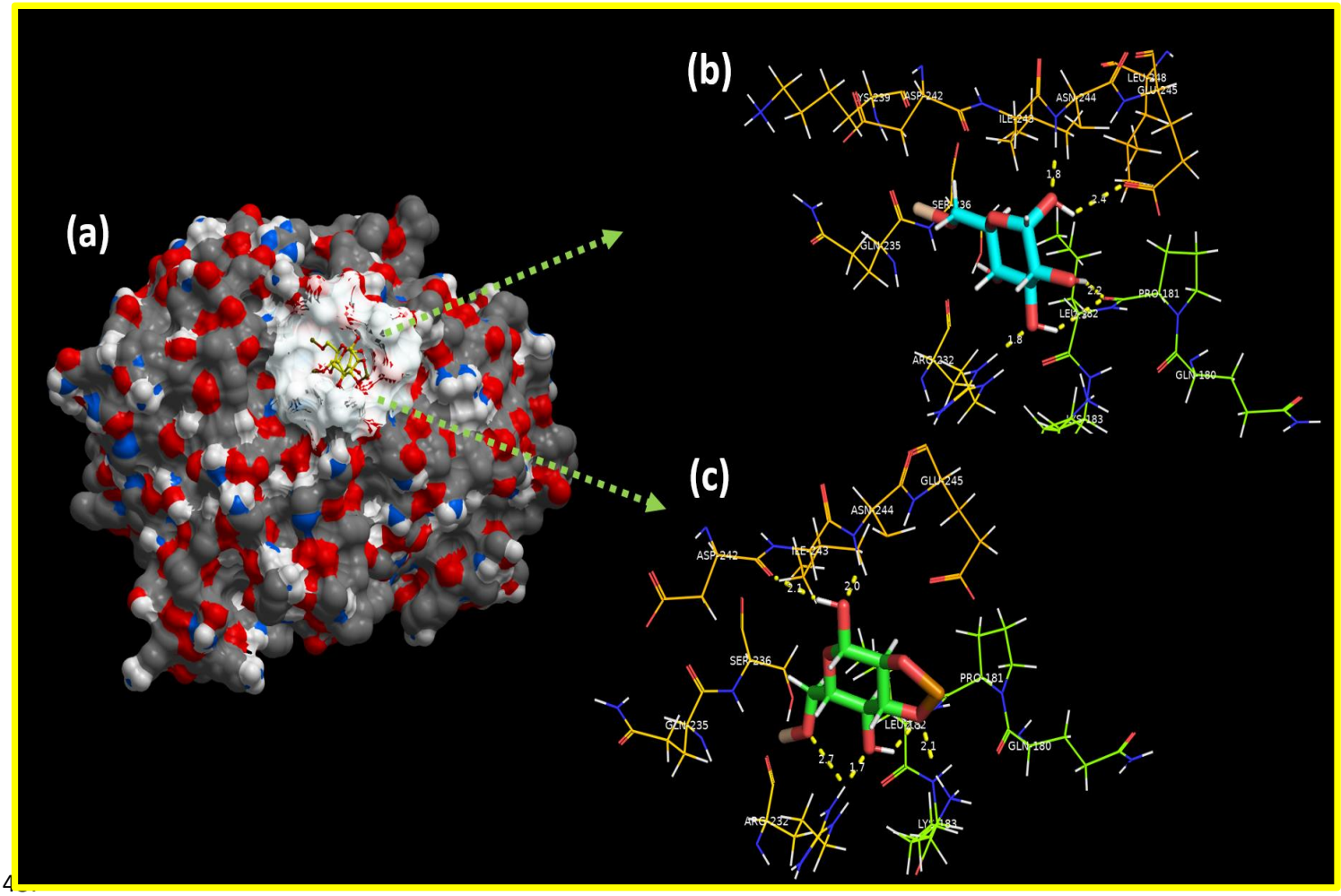

Fig 10: (a). Nanocomposites-β-lactamase$_{E.coli}$ docked complexes (superimposed), **(b).** SrO-starch-β-lactamase$_{E.coli}$ complex, (c). Te/ SrO-starch-β-lactamase$_{E.coli}$ complex

For the case of DNA gyrase$_{E.coli}$, the top tanked docked conformation with SrO-starch having the lowest binding score (i.e., -8.901 kcal/mol) revealed H-bonding interactions with Gly77 (2.2 Å), Asp73 (2.5 and 2.7 Å), and Thr165 (2.3 and 1.9 Å) while Asn46, Glu50 and Ile78 showed C-H interactions as shown in Fig. 11. Similarly, the binding tendency and interaction pattern revealed by Te/SrO-starch nanocomposite are also good with an overall binding score of -9.799 kcal/mol. Three amino acid residues interact through H-bond, i.e., Asp73 (2.2 Å), Thr165 (2.2 and 1.7 Å) and Gly77 (2.1 Å), as depicted in Fig. 11.

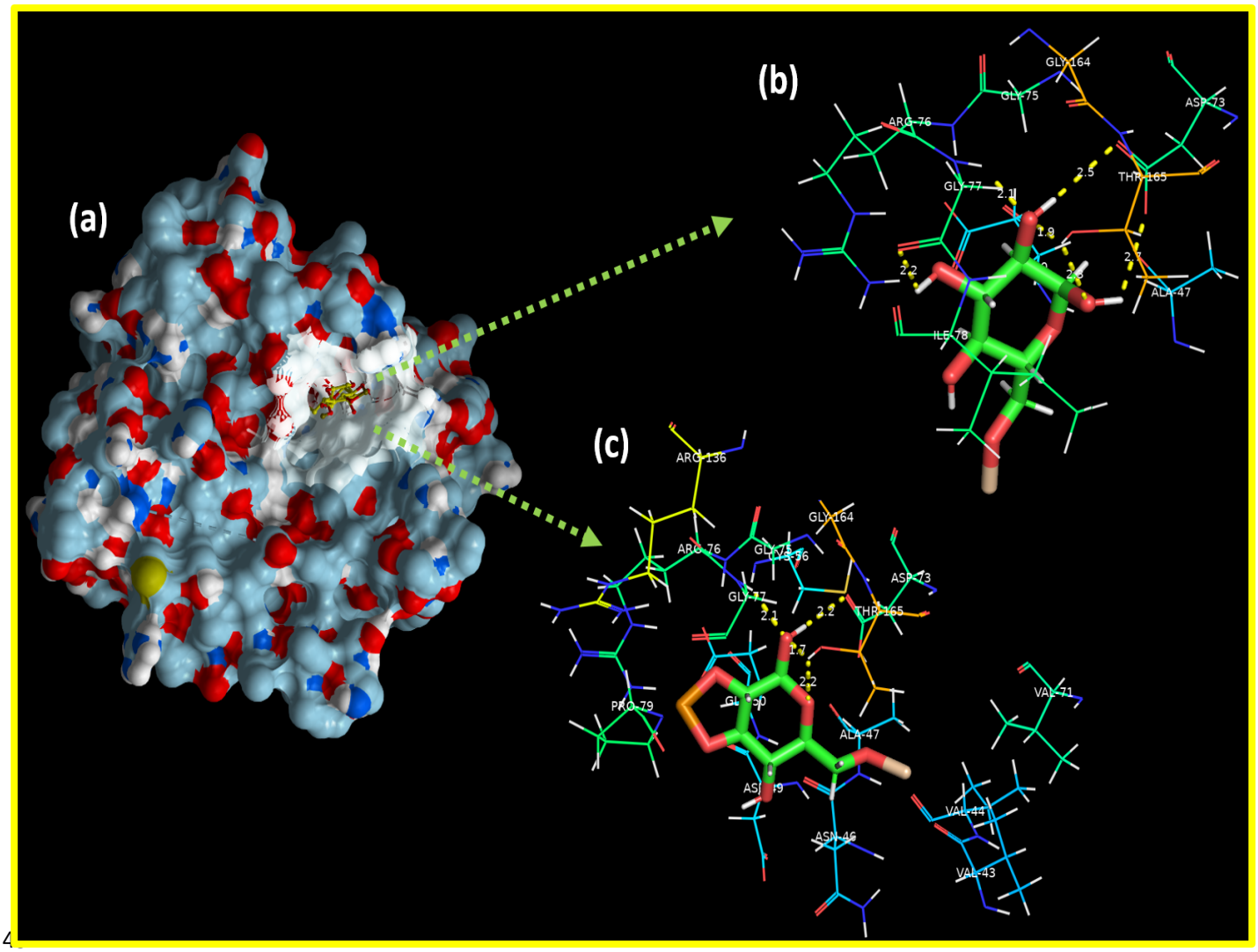

Fig. 11: (a). Nanocomposites-DNA Gyrase$_{E.coli}$ docked complexes (superimposed), **(b).** SrO-starch-DNA Gyrase$_{E.coli}$ complex, (c). Te/SrO-starch-DNA Gyrase$_{E.coli}$ complex

In silico molecular docking studies suggested these nanocomposites as possible inhibitors of *β*-lactamase$_{E.coli}$ and DNA Gyrase$_{E.coli}$ that need further exploration.

4. CONCLUSION

This study successfully prepared SrO, starch, SrO-starch composite, and various Te doping concentrations (2 and 4 %) in SrO-starch composite nanoparticles through the chemical co-

precipitation method. Various characterizations have been employed to investigate structural, morphological and optical analysis. Various phases have been confirmed the pristine, SrO-starch composite and Te doped composite samples represent enhanced crystallinity through XRD analysis and crystalline size decrease with increasing concentration from 26.18-5.96 nm. The appearance of Sr-O has been characterized by FTIR evaluation. SAED pattern confirms that the prepared samples are crystalline and well-matched with XRD consequences. EDS interpretation confirms the successful preparation of pure and doped samples with Sr, O, and Te atoms. An increase in energy band gap from 4.23-4.59 eV was observed for pure and doped samples, showing the blue band emission spectra through UV-vis spectrophotometry. PL spectra represent excitons recombination and rate transfer of electron and hole. PL spectra indicate the reduction rate of recombination for increasing the concentration of doped material exhibits enhancement in catalytic activity has been affirmed by measured results. The structure and morphology of synthesized nanoparticles have been clarified through FE-SEM and TEM analysis. Interlayer spacing of pure and doped samples 0.25 nm and 0.28 nm was calculated via HRTEM images. Catalytic activity indicates a rapid enhancement in dye degradation of MB. Dye degradation has been effectively achieved with the optimum concentration of doping of Te in neutral (84.76%), basic (86.32%), and acidic (89.57%) mediums for a 4% Te-doped SrO-starch composite. The highest catalytic degradation has been observed in acidic (91.42%) medium for 2% Te-doped SrO-starch composite. The measured experimental results show that optimum concentration (2%) of Te-doped SrO-starch composite has been used for rapid enhancement in catalytic dye degradation and as a superior catalyst replace conventional wastewater management approach. Prepared NPs exhibit excellent antimicrobial activity against *S. aureus* bacteria compared to *E. coli*. 4% Te-doped SrO-starch composite NPs show excellent efficiency

against *S. aureus* with an inhibition zone of 9.30 mm as compared to *E. coli* with a measured zone of inhibition of 3.25 mm. *In silico* studies showed good agreement with in vitro bactericidal activities and suggested both SrO-starch and Te-doped SrO-starch composite as a potential inhibitor of β-lactamase$_{E.coli}$ and DNA Gyrase$_{E.coli}$.

ACKNOWLEDGMENT: Authors are thankful to HEC, Pakistan through project NRPU-20-17615.

CONFLICT OF INTEREST: The authors declare "no conflict of interest."

AVAILABILITY OF DATA: Data available on demand

REFERENCES

[1] A.L. Srivastav, Chemical fertilizers and pesticides: role in groundwater contamination, in: Agrochem. Detect. Treat. Remediat., Butterworth-Heinemann, 2020: pp. 143–159. https://doi.org/10.1016/b978-0-08-103017-2.00006-4.

[2] D. Zhao, Y. Yu, J.P. Chen, Treatment of lead contaminated water by a PVDF membrane that is modified by zirconium, phosphate and PVA, Water Res. 101 (2016) 564–573. https://doi.org/10.1016/j.watres.2016.04.078.

[3] M.M. Mekonnen, A.Y. Hoekstra, Sustainability: Four billion people facing severe water scarcity, Sci. Adv. 2 (2016) 23. https://doi.org/10.1126/sciadv.1500323.

[4] M. Kummu, J.H.A. Guillaume, H. De Moel, S. Eisner, M. Flörke, M. Porkka, S. Siebert, T.I.E. Veldkamp, P.J. Ward, The world's road to water scarcity: Shortage and stress in the 20th century and pathways towards sustainability, Sci. Rep. 6 (2016) 1-16.

548 https://doi.org/10.1038/srep38495.

549 [5] S. Sharma, A. Bhattacharya, Drinking water contamination and treatment techniques,
550 Appl. Water Sci. 7 (2017) 1043–1067. https://doi.org/10.1007/s13201-016-0455-7.

551 [6] D. Cambié, C. Bottecchia, N.J.W. Straathof, V. Hessel, T. Noël, Applications of
552 Continuous-Flow Photochemistry in Organic Synthesis, Material Science, and Water
553 Treatment, Chem. Rev. 116 (2016) 10276–10341.
554 https://doi.org/10.1021/acs.chemrev.5b00707.

555 [7] R. Sankaranarayanan, J. Ferlay, Worldwide burden of gynaecological cancer: The size of
556 the problem, Best Pract. Res. Clin. Obstet. Gynaecol. 20 (2006) 207–225.
557 https://doi.org/10.1016/j.bpobgyn.2005.10.007.

558 [8] H. Li, H. Shen, L. Duan, R. Liu, Q. Li, Q. Zhang, X. Zhao, Enhanced photocatalytic
559 activity and synthesis of ZnO nanorods/MoS2 composites, Superlattices Microstruct. 117
560 (2018) 336–341. https://doi.org/10.1016/j.spmi.2018.03.028.

561 [9] V. Melinte, L. Stroea, A.L. Chibac-Scutaru, Polymer nanocomposites for photocatalytic
562 applications, Catalysts. 9 (2019) 986. https://doi.org/10.3390/catal9120986.

563 [10] B. Tabah, A.P. Nagvenkar, N. Perkas, A. Gedanken, Solar-Heated Sustainable Biodiesel
564 Production from Waste Cooking Oil Using a Sonochemically Deposited SrO Catalyst on
565 Microporous Activated Carbon, Energy & Fuels. 31 (2017) 6228–6239.
566 https://doi.org/10.1021/acs.energyfuels.7b00932.

567 [11] M.M. Rahman, M.M. Hussain, A.M. Asiri, A novel approach towards hydrazine sensor
568 development using SrO·CNT nanocomposites, RSC Adv. 6 (2016) 65338–65348.

https://doi.org/10.1039/c6ra11582a.

[12] M. Alavi, A. Nokhodchi, An overview on antimicrobial and wound healing properties of ZnO nanobiofilms, hydrogels, and bionanocomposites based on cellulose, chitosan, and alginate polymers, Carbohydr. Polym. 227 (2020) 260-269. https://doi.org/10.1016/j.carbpol.2019.115349.

[13] H. Jacobs, J.A. Delcour, Hydrothermal Modifications of Granular Starch, with Retention of the Granular Structure: A Review, J. Agric. Food Chem. 46 (1998) 2895–2905. https://doi.org/10.1021/jf980169k.

[14] S.C. Alcázar-Alay, M.A.A. Meireles, Physicochemical properties, modifications and applications of starches from different botanical sources, Food Sci. Technol. 35 (2015) 215–236. https://doi.org/10.1590/1678-457X.6749.

[15] K. Devi, S. Haripriya, Pasting behaviors of starch and protein in soy flour-enriched composite flours on quality of biscuits, J. Food Process. Preserv. 38 (2014) 116–124. https://doi.org/10.1111/j.1745-4549.2012.00752.x.

[16] J. Firdaus, E. Sulistyaningsih, A. Subagio, Resistant Starch Modified Cassava Flour (MOCAF) improves insulin resistance, Asian J. Clin. Nutr. 10 (2018) 32–36. https://doi.org/10.3923/ajcn.2018.32.36.

[17] J.Y. Kim, S.T. Lim, Preparation of nano-sized starch particles by complex formation with n-butanol, Carbohydr. Polym. 76 (2009) 110–116. https://doi.org/10.1016/j.carbpol.2008.09.030.

[18] J.A. Pellicer, M.I. Fortea, J. Trabal, M.I. Rodríguez-López, C. Carazo-Díaz, J.A.

590 Gabaldón, E. Núñez-Delicado, Optimization of the microencapsulation of synthetic
591 strawberry flavour with different blends of encapsulating agents using spray drying,
592 Powder Technol. 338 (2018) 591–598. https://doi.org/10.1016/j.powtec.2018.07.080.

593 [19] G.C. Hoover, D.S. Seferos, Photoactivity and optical applications of organic materials
594 containing selenium and tellurium, Chem. Sci. 10 (2019) 9182–9188.
595 https://doi.org/10.1039/c9sc04279b.

596 [20] A.P. Mirgorodsky, T. Merle-Méjean, J.C. Champarnaud, P. Thomas, B. Frit, Dynamics
597 and structure of TeO2 polymorphs: Model treatment of paratellurite and tellurite; Raman
598 scattering evidence for new γ- and δ-phases, J. Phys. Chem. Solids. 61 (2000) 501–509.
599 https://doi.org/10.1016/S0022-3697(99)00263-2.

600 [21] V. Nagarajan, R. Chandiramouli, TeO2 nanostructures as a NO2 sensor: DFT
601 investigation, Comput. Theor. Chem. 1049 (2014) 20–27.
602 https://doi.org/10.1016/j.comptc.2014.09.009.

603 [22] S. Hati, N. Patel, S. Mandal, Comparative Growth Behaviour and Biofunctionality of
604 Lactic Acid Bacteria During Fermentation of Soy Milk and Bovine Milk, Probiotics
605 Antimicrob. Proteins. 10 (2018) 277–283. https://doi.org/10.1007/s12602-017-9279-5.

606 [23] A. Haider, M. Ijaz, M. Imran, M. Naz, H. Majeed, J.A. Khan, M.M. Ali, M. Ikram,
607 Enhanced bactericidal action and dye degradation of spicy roots' extract-incorporated
608 fine-tuned metal oxide nanoparticles, Appl. Nanosci. 10 (2020) 1095–1104.
609 https://doi.org/10.1007/s13204-019-01188-x.

610 [24] S. Stankic, S. Suman, F. Haque, J. Vidic, Pure and multi metal oxide nanoparticles:

Synthesis, antibacterial and cytotoxic properties, J. Nanobiotechnology. 14 (2016) 1-20. https://doi.org/10.1186/s12951-016-0225-6.

[25] D. Kryukova, A. Sokolov, M. Maksimov, Pharmacology of inhibitor-protected beta-lactam agents, Novejshie Zarubezhnye i Otechestvennye Lek. Prep. Farmakoter. Farmakodinamika, Farmakokinet. (Newest Foreign Domest. Prep. Pharmacother. Pharmacodyn. Pharmacokinet. (2020) 53–69. https://doi.org/10.33920/med-06-2003-05.

[26] F. Ushiyama, H. Amada, T. Takeuchi, N. Tanaka-Yamamoto, H. Kanazawa, K. Nakano, M. Mima, A. Masuko, I. Takata, K. Hitaka, K. Iwamoto, H. Sugiyama, N. Ohtake, Lead Identification of 8-(Methylamino)-2-oxo-1,2-dihydroquinoline Derivatives as DNA Gyrase Inhibitors: Hit-to-Lead Generation Involving Thermodynamic Evaluation, ACS Omega. 5 (2020) 10145–10159. https://doi.org/10.1021/acsomega.0c00865.

[27] S. Barelier, O. Eidam, I. Fish, J. Hollander, F. Figaroa, R. Nachane, J.J. Irwin, B.K. Shoichet, G. Siegal, Increasing chemical space coverage by combining empirical and computational fragment screens, ACS Chem. Biol. 9 (2014) 1528–1535. https://doi.org/10.1021/cb5001636.

[28] P. Panchaud, T. Bruyère, A.C. Blumstein, D. Bur, A. Chambovey, E.A. Ertel, M. Gude, C. Hubschwerlen, L. Jacob, T. Kimmerlin, T. Pfeifer, L. Prade, P. Seiler, D. Ritz, G. Rueedi, Discovery and Optimization of Isoquinoline Ethyl Ureas as Antibacterial Agents, J. Med. Chem. 60 (2017) 3755–3775. https://doi.org/10.1021/acs.jmedchem.6b01834.

[29] R. Abagyan, M. Totrov, Biased probability Monte Carlo conformational searches and electrostatic calculations for peptides and proteins, J. Mol. Biol. 235 (1994) 983–1002. https://doi.org/10.1006/jmbi.1994.1052.

[30] H. Liu, L. Yu, F. Xie, L. Chen, Gelatinization of cornstarch with different amylose/amylopectin content, Carbohydr. Polym. 65 (2006) 357–363. https://doi.org/10.1016/j.carbpol.2006.01.026.

[31] J. Jane, Current Understanding on Starch Granule Structures, J. Appl. Glycosci. 53 (2006) 205–213. https://doi.org/10.5458/jag.53.205.

[32] J. Karkalas, X. Qi, R.F. Tester, Starch-composition, fine structure and architecture, J. Cereal Sci. 39 (2004) 151–165. https://www.sciencedirect.com/science/article/pii/S0733521003001139.

[33] M. Todica, E.M. Nagy, C. Niculaescu, O. Stan, N. Cioica, C.V. Pop, XRD investigation of some thermal degraded starch based materials, J. Spectrosc. 2016 (2016) 6. https://doi.org/10.1155/2016/9605312.

[34] T. Athar, Synthesis and Characterization of Strontium Oxide Nanoparticles via Wet Process, Mater. Focus. 2 (2013) 450–453. https://doi.org/10.1166/mat.2013.1121.

[35] J.J.G. van Soest, H. Tournois, D. de Wit, J.F.G. Vliegenthart, Short-range structure in (partially) crystalline potato starch determined with attenuated total reflectance Fourier-transform IR spectroscopy, Carbohydr. Res. 279 (1995) 201–214. https://doi.org/10.1016/0008-6215(95)00270-7.

[36] J.M. Fang, P.A. Fowler, C. Sayers, P.A. Williams, The chemical modification of a range of starches under aqueous reaction conditions, Carbohydr. Polym. 55 (2004) 283–289. https://doi.org/10.1016/j.carbpol.2003.10.003.

[37] A.M. Nzenguet, M. Aqlil, Y. Essamlali, O. Amadine, A. Snik, M. Larzek, M. Zahouily,

654 Novel bionanocomposite films based on graphene oxide filled starch/polyacrylamide
655 polymer blend: structural, mechanical and water barrier properties, J. Polym. Res. 25
656 (2018) 1-13. https://doi.org/10.1007/s10965-018-1469-7.

657 [38] R. Cisek, D. Tokarz, L. Kontenis, V. Barzda, M. Steup, Polarimetric second harmonic
658 generation microscopy: An analytical tool for starch bioengineering, Starch-St◆rke. 70
659 (2018) 1700031. https://doi.org/10.1002/star.201700031.

660 [39] V.K. Shivaraju, S. Vallayil Appukuttan, S.K. Sunny Kumar, The Influence of Bound
661 Water on the FTIR Characteristics of Starch and Starch Nanocrystals Obtained from
662 Selected Natural Sources, Starch-St◆rke. 71 (2019) 1700026.
663 https://doi.org/10.1002/star.201700026.

664 [40] F. Boccuzzi, A. Chiorino, S. Tsubota, M. Haruta, FTIR study of carbon monoxide
665 oxidation and scrambling at room temperature over gold supported on ZnO and TiO2. 2, J.
666 Phys. Chem. 100 (1996) 3625–3631. https://doi.org/10.1021/jp952259n.

667 [41] D.E. Newbury, Mistakes encountered during automatic peak identification of minor and
668 trace constituents in electron-excited energy dispersive X-ray microanalysis, Scanning. 31
669 (2009) 91–101. https://doi.org/10.1002/sca.20151.

670 [42] K.K. M., B. K., N. G., S. B., V. A., Plasmonic resonance nature of Ag-Cu/TiO2
671 photocatalyst under solar and artificial light: Synthesis, characterization and evaluation of
672 H2O splitting activity, Appl. Catal. B Environ. 199 (2016) 282–291.
673 https://doi.org/10.1016/j.apcatb.2016.06.050.

674 [43] N. Yamashita, Photoluminescence spectra of the Eu2+ center in SrO:Eu, J. Lumin. 59

675 (1994) 195–199. https://doi.org/10.1016/0022-2313(94)90041-8.

676 [44] M. Valodkar, S. Modi, A. Pal, S. Thakore, Synthesis and anti-bacterial activity of Cu, Ag
677 and Cu-Ag alloy nanoparticles: A green approach, Mater. Res. Bull. 46 (2011) 384–389.
678 https://doi.org/10.1016/j.materresbull.2010.12.001.

679 [45] M. Aqeel, M. Rashid, M. Ikram, A. Haider, S. Naz, J. Haider, A. Ul-Hamid, A. Shahzadi,
680 Photocatalytic, dye degradation, and bactericidal behavior of Cu-doped ZnO nanorods and
681 their molecular docking analysis, Dalt. Trans. 49 (2020) 8314–8330.
682 https://doi.org/10.1039/d0dt01397h.

683 [46] A. Shahpal, M. Aziz Choudhary, Z. Ahmad, An investigation on the synthesis and
684 catalytic activities of pure and Cu-doped zinc oxide nanoparticles, Cogent Chem. 3 (2017)
685 1301241. https://doi.org/10.1080/23312009.2017.1301241.

686 [47] A.A. Fairuzi, N.N. Bonnia, R.M. Akhir, M.A. Abrani, H.M. Akil, Degradation of
687 methylene blue using silver nanoparticles synthesized from imperata cylindrica aqueous
688 extract, in: IOP Conf. Ser. Earth Environ. Sci., Institute of Physics Publishing, (2018)
689 012018. https://doi.org/10.1088/1755-1315/105/1/012018.

690 [48] M. Ikram, T. Inayat, A. Haider, A. Ul-Hamid, J. Haider, W. Nabgan, A. Saeed, A.
691 Shahbaz, S. Hayat, K. Ul-Ain, A.R. Butt, Graphene Oxide-Doped MgO Nanostructures
692 for Highly Efficient Dye Degradation and Bactericidal Action, Nanoscale Res. Lett. 16
693 (2021) 1–11. https://doi.org/10.1186/s11671-021-03516-z.

694 [49] S.K. Jesudoss, J.J. Vijaya, L.J. Kennedy, P.I. Rajan, H.A. Al-Lohedan, R.J. Ramalingam,
695 K. Kaviyarasu, M. Bououdina, Studies on the efficient dual performance of Mn1–

xNixFe2O4 spinel nanoparticles in photodegradation and antibacterial activity, J. Photochem. Photobiol. B Biol. 165 (2016) 121–132. https://doi.org/10.1016/j.jphotobiol.2016.10.004.

[50] G.R. Navale, C.S. Rout, K.N. Gohil, M.S. Dharne, D.J. Late, S.S. Shinde, Oxidative and membrane stress-mediated antibacterial activity of WS2 and rGO-WS2 nanosheets, RSC Adv. 5 (2015) 74726–74733. https://doi.org/10.1039/c5ra15652a.

[51] Z.N. Kayani, M. Sahar, S. Riaz, S. Naseem, Z. Saddiqe, Enhanced magnetic, antibacterial and optical properties of Sm doped ZnO thin films: Role of Sm doping, Opt. Mater. (Amst). 108 (2020). https://doi.org/10.1016/j.optmat.2020.110457.

[52] N. Rajiv Chandar, S. Agilan, R. Thangarasu, N. Muthukumarasamy, J. Chandrasekaran, S. Arunachalam, S.R. Akshaya, Elucidation of efficient dual performance in photodegradation and antibacterial activity by a promising candidate Ni-doped MoO3 nanostructure, J. Sol-Gel Sci. Technol. 100 (2021) 451–465. https://doi.org/10.1007/s10971-020-05382-0.

[53] A. Robert Xavier, A.T. Ravichandran, K. Ravichandran, S. Mantha, D. Ravinder, Sm doping effect on structural, morphological, luminescence and antibacterial activity of CdO nanoparticles, J. Mater. Sci. Mater. Electron. 27 (2016) 11182–11187. https://doi.org/10.1007/s10854-016-5237-3.

[54] B. Ahmed, A. Hashmi, M.S. Khan, J. Musarrat, ROS mediated destruction of cell membrane, growth and biofilms of human bacterial pathogens by stable metallic AgNPs functionalized from bell pepper extract and quercetin, Adv. Powder Technol. 29 (2018) 1601–1616. https://doi.org/10.1016/j.apt.2018.03.025.

[55] B. Ahmed, B. Solanki, A. Zaidi, M.S. Khan, J. Musarrat, Bacterial toxicity of biomimetic green zinc oxide nanoantibiotic: insights into ZnONP uptake and nanocolloid-bacteria interface, Toxicol. Res. (Camb). 8 (2019) 246–261. https://doi.org/10.1039/C8TX00267C.

[56] K. Ali, B. Ahmed, S.M. Ansari, Q. Saquib, A.A. Al-Khedhairy, S. Dwivedi, M. Alshaeri, M.S. Khan, J. Musarrat, Comparative in situ ROS mediated killing of bacteria with bulk analogue, Eucalyptus leaf extract (ELE)-capped and bare surface copper oxide nanoparticles, Mater. Sci. Eng. C. 100 (2019) 747–758. https://doi.org/10.1016/j.msec.2019.03.012.

[57] K. Ali, B. Ahmed, M.S. Khan, J. Musarrat, Differential surface contact killing of pristine and low EPS Pseudomonas aeruginosa with Aloe vera capped hematite (α-Fe2O3) nanoparticles, J. Photochem. Photobiol. B Biol. 188 (2018) 146–158. https://doi.org/10.1016/j.jphotobiol.2018.09.017.

[58] M. Haroon, A. Zaidi, B. Ahmed, A. Rizvi, M.S. Khan, J. Musarrat, Effective Inhibition of Phytopathogenic Microbes by Eco-Friendly Leaf Extract Mediated Silver Nanoparticles (AgNPs), Indian J. Microbiol. 59 (2019) 273–287. https://doi.org/10.1007/s12088-019-00801-5.

[59] P. Iyyappa Rajan, J. Judith Vijaya, S.K. Jesudoss, K. Kaviyarasu, L. John Kennedy, R. Jothiramalingam, H.A. Al-Lohedan, M.A. Vaali-Mohammed, Green-fuel-mediated synthesis of self-assembled NiO nano-sticks for dual applications-photocatalytic activity on Rose Bengal dye and antimicrobial action on bacterial strains, Mater. Res. Express. 4 (2017) 085030. https://doi.org/10.1088/2053-1591/aa7e3c.

[60] A. Haider, M. Ijaz, S. Ali, J. Haider, M. Imran, H. Majeed, I. Shahzadi, M.M. Ali, J.A.

Khan, M. Ikram, Green Synthesized Phytochemically (Zingiber officinale and Allium sativum) Reduced Nickel Oxide Nanoparticles Confirmed Bactericidal and Catalytic Potential, Nanoscale Res. Lett. 15 (2020) 1-11. https://doi.org/10.1186/s11671-020-3283-5.

[61] M.K. Rai, S.D. Deshmukh, A.P. Ingle, A.K. Gade, Silver nanoparticles: The powerful nanoweapon against multidrug-resistant bacteria, J. Appl. Microbiol. 112 (2012) 841–852. https://doi.org/10.1111/j.1365-2672.2012.05253.x.

[62] N.Y. Lee, W.C. Ko, P.R. Hsueh, Nanoparticles in the treatment of infections caused by multidrug-resistant organisms, Front. Pharmacol. 10 (2019) 1153. https://doi.org/10.3389/fphar.2019.01153.

[63] A. Thill, O. Zeyons, O. Spalla, F. Chauvat, J. Rose, M. Auffan, A.M. Flank, Cytotoxicity of CeO2 nanoparticles for Escherichia coli. Physico-chemical insight of the cytotoxicity mechanism, Environ. Sci. Technol. 40 (2006) 6151–6156. https://doi.org/10.1021/es060999b.

[64] S.Y. Essack, The development of β-lactam antibiotics in response to the evolution of β-lactamases, Pharm. Res. 18 (2001) 1391–1399. https://doi.org/10.1023/A:1012272403776.

ABSTRACT

A chemical co-precipitation route was used to synthesize novel strontium oxide (SrO), SrO-starch composite and various tellurium (Te) concentrations were incorporated in SrO-starch composite. This study aims to enhance the catalytic activities and bactericidal behavior of SrO, SrO-starch composite with different percentage concentrations of Te doping and a fixed amount of starch nanoparticles. XRD affirmed that the dopant contribution was investigated to improve crystallinity. Surface morphological characteristics and elemental composition evaluation were determined using an FE-SEM and EDS exhibit a doping concentration of an element in the synthesized products. The configuration of Sr–O–Sr bonds and molecular vibrations has been indicated by FTIR spectra. In addition, dye degradation of prepared samples was investigated through catalytic activity (CA) in the existence of $NaBH_4$ act as a reduction representative. The Te-doped SrO-starch composite indicates superior catalytic activity and shows a degradation of Methylene blue dye (91.4%) in an acidic medium. The synthesis nanocatalyst demonstrated impressive antibacterial activity against *Staphylococcus aureus* (*S. aureus*) at high and low concentrations exhibiting zones of inhibition 9.30 mm as compared to ciprofloxacin. Furthermore, molecular docking studies of synthesized nanocomposites were performed against selected enzyme targets, i.e., β-lactamase$_{E.coli}$ and DNA Gyrase$_{E.coli}$.